Functional dynamics of brain networks associated with carry-over effects of negative events on subsequent resting state.

Julian Gaviria[1,2,3], Gwladys Rey[3], Thomas Bolton[4,5], Dimitri Van de Ville[4,5], Patrik Vuilleumier[1,2,3]

[1]Laboratory for Behavioral Neurology and Imaging of Cognition; [2]Department of Fundamental Neurosciences, University of Geneva, Geneva, Switzerland; [3] Swiss center for Affective Sciences, University of Geneva; [4]Medical Image Processing Lab, Institute of Bioengineering/Center for Neuroprosthetics, École Polytechnique Fédérale de Lausanne (EPFL), Geneva, Switzerland; [5]Department of Radiology and Medical Informatics, University of Geneva, Geneva, Switzerland

Address correspondence to Julian Gaviria. Campus Biotech, 9 Chemin des Mines, 1202 Genève, Switzerland; E-mail: Julian(dot)GaviriaLopez(at)unige(dot)ch; Tel: +41779388860

Brain networks; negative emotions; dynamic functional connectivity (dFC); task-rest interaction; co-activation patterns (CAPs)

Abstract

Distributed brain areas are engaged both during and following the elicitation of emotional experiences. Previous studies suggest that transient emotions may cause a prolonged impact (or inertia) on brain states, with corresponding changes in subjective affect and mood. To investigate the functional dynamics and reciprocal interactions among brain networks underlying these effects, we quantified co-activation patterns (CAPs) by recording functional magnetic resonance imaging (fMRI) during sad movies and subsequent resting periods. CAPs overlapping with the visual (VIS), default mode (DMN), central executive (CEN), and frontoparietal control (FPCN) networks showed not only distinctive effects of negative emotion on their spatiotemporal expression in both movie and rest periods, but also different reciprocal relationships among them in transitions from movie to rest. While FPCN and DMN expression increased during and after negative movies, respectively, FPCN occurrences during the movie predicted lower DMN and higher CEN expression during subsequent rest after neutral movies, but this relationship was reversed after negative movies. Changes in FPCN and DMN activity correlated with more negative subjective affect. These findings provide new insights into the functional dynamics and interactions of intrinsic brain networks, highlighting a major role of FPCN in emotion elicitation processes with prolonged impact on DMN activity in subsequent rest, presumably involved in emotion regulation and restoration of homeostatic balance after negative events.

Introduction

Abundant work in neuroscience shows that functional brain activity and connectivity is dynamically organized across several distributed networks with simultaneous ongoing fluctuations and selective reciprocal interactions (e.g., correlated or anticorrelated) according to current behavioral demands (1). These spatiotemporal fluctuations in intrinsic functional networks (IFNs) can be observed during particular tasks as well as during rest. Among IFNs, the default mode network (DMN) encompasses a set of midline cortical areas, including precuneus and medial prefrontal cortices (MPFC) that are usually active during mind-wandering in "task-off" conditions at rest (2). However, this network might also play a more specific and active role in integrative functions related to higher-level aspects of self-awareness and introspection (3). The DMN activity is associated with self-reflective and memory-related task conditions (4) and typically anticorrelates with activity of the fronto-parietal control network (FPCN), which is recruited by externally directed attention (5). DMN activity also fluctuates between periods of positive and negative correlation with the central executive network (CEN) and saliency networks (SN), indicating switches between different cognitive processing modes (6). In addition, there is evidence that the DMN interactions are modulated by emotional information and current mood (7, 8). However, its exact role in affective processes is unclear.

In the present study, we investigated how IFNs dynamically reconfigure and reciprocally interact with each other in response to negative emotional episodes, both during emotional stimulation itself and during the recovery period following such stimulation. Dynamic reciprocal interactions among IFNs dovetails with a general theoretical framework of affective phenomena (9) according to which emotions emerge from a coordinated recruitment of component processes, each underpinned by distinct neural systems, whose synchronization is triggered by behaviorally relevant events and promotes adaptive changes in the organism (10, 11). Evidence for affective influences on DMN activity and its interaction with other networks comes from several observations (12, 13), but their functional significance remains unresolved. A down-regulation of within-DMN connectivity was reported in healthy participants during sad mood induction through self-generated memories (14) or movies (15), while disturbances of DMN connectivity are observed in clinical mood disorders such as depression and bipolar disease (16, 17). Dynamic shifts in the balance between DMN and SN are also thought to mediate adaptive responses to acute stressors, promoting higher vigilance and fear (18). Furthermore, changes in the activation and spatial configuration of DMN at rest can be modified by preceding cognitive (19) or affective (8, 20) task conditions. In particular, exposure to emotional stimuli or rewards has been found to induce long-lasting changes in brain activity and connectivity, overlapping with DMN, SN, and FPCN, which persist even after termination of the eliciting event itself, e.g., during subsequent

resting state (14, 15, 20, 21). Such carry-over effects of emotions on neural activity at rest might reflect spontaneous self-regulation mechanisms restoring a homeostatic balance in brain state (8, 20), and is enhanced by individual anxiety levels (22), consistent with behavioral evidence for maladaptive emotional inertia (23) and ruminative processing triggered by negative events in psychopathological conditions (24). In accordance with this idea, cognitive reappraisal of negative audiovisual stimuli (compared to freely watching) may produce not only a reduced neural response to these stimuli in limbic areas (e.g., amygdala), but also an increased activation of cortical networks overlapping with DMN and FPCN during both stimulus presentation and subsequent rest (25).

However, previous studies on emotion-responsive networks and emotion after-effects generally focused on *static* connectivity patterns, temporally summarized at the whole-brain level, either during emotional stimulation or during resting conditions following emotional stimulation (compared to neutral). They did not characterize the *dynamics* of changes in specific IFNs during these different periods; nor did they examine how these changes may emerge from interactions *between* different IFNs simultaneously modulated by emotional state. Hence, these studies do not offer any mechanistic insights into how IFNs dynamically unfold during and after emotions, and how their acute engagement by an emotion-eliciting event may influence the subsequent return to a normal resting baseline after termination of this event (26).

To directly address these issues, we designed a novel emotion elicitation paradigm where participants freely viewed sad (vs. neutral) movies followed by a resting state period. To uncover IFNs differentially engaged during emotional movies and their subsequent carry-over at rest, as well as their reciprocal relationships, we leveraged an innovative methodology allowing us to track dynamic functional connectivity (dFC) with co-activation pattern (CAP) analysis (27, 28). By delineating brain-wide CAPs modulated by emotion in movie and rest periods, we asked the following questions: (1) what is the carry-over impact of negative events on the dynamics and reciprocal interactions of brain networks and how do they unfold in time beyond these events, i.e., in the aftermath of emotion during subsequent rest (see Fig 1A); (2) whether changes in brain states subsequent to negative emotions, particularly in DMN and interconnected networks, are associated with changes in subjective affective state; and (3) how is the carry-over effect emotion on resting IFNs related to the occurrence of specific activity patterns during the preceding emotional events. By characterizing the spatiotemporal features of IFNs during and after negative affect induction, our study provides new insights on the brain dynamics of emotional responses and may help identify novel neurobiological markers for negative affect experience and regulation, possibly altered in clinical populations with anxiety and mood disorders.

Materials and Methods

Participants

Twenty right-handed, French-speaking female volunteers (mean age= 23.2 ± 4.3) were contacted via posters and online advertisement. They all provided written informed consent according to the Geneva University Hospital Ethics Committee. Only female participants were recruited because pilot testing suggested stronger emotional induction in women, compared to male, particularly with the movie clips used here (see Supplementary methods). Controlled inclusion criteria were: no history of neurological and psychiatric diseases; known menstrual phase and no contraceptive method to rule out hormonal effects on emotional processing (29) or functional connectivity (30, 31); no major head movement during the scanning sessions (<1.5 mm in all axes). Scanning was scheduled for each participant in the early stage of the menstrual follicular phase, when the levels of estradiol and progesterone hormones are moderate (32, 33). Nicotine and caffeine consumption was prohibited 10 hours before scanning.

Behavioral paradigm

Initially, the participants filled the French version of the PANAS questionnaires. This was followed by an fMRI experiment with a repeated measure design. The scanning session comprised two experimental "contexts". One context included an audio-visual clip (5 min) with sad emotional content ("negative movie" condition), followed by a resting period (5 min) ("negative rest" condition). As a control for affective valence, the second experimental context comprised non-emotional video clip (5 min) ("neutral movie"), followed by another resting period ("neutral" rest condition) (5min). Participants were instructed to keep their eyes opened and to stay awake across the resting periods. This was controlled by an eye-tracking device both online and offline. Importantly, the presentation order of the two contexts was counterbalanced across participants (see Fig. 1A., for schematic overview of the paradigm design). At the end of each experimental scanning session (i.e., "neutral" and "negative"), further PANAS scores and emotion questionnaires about the movies were also filled. Approximately 20 minutes elapsed between the end of one experimental context and the starting of the next one. Additional information on movies and subjective ratings is provided in the SI material.

MRI data acquisition

Anatomical and functional whole-brain MRI data were acquired with a 3T scanner (Siemens TIM Trio) at the Brain & Behavior Laboratory, University of Geneva. A multiband-sequence was implemented, with a voxel size of 2mm isometric and a TR of 1.3s (see SI for further description of both data acquisition and preprocessing).

fMRI brain analysis.

The present study focused on the interaction of transient IFNs over time observed during stimulation with negative movies and following stimulation. To this aim, our approach comprised three successive stages: (1) GLM-based identification of brain regions of interest (ROIs) with emotion-related activation to define connectivity seeds. (2) CAP-based analysis of dynamic functional connectivity to identify brain networks differentially engaged by experimental conditions. (3) In-depth analysis of functional interactions among the emotionally-relevant CAPs, either between themselves or between experimental phases, in both affective contexts.

GLM-based ROIs identification

The GLM analysis assessed BOLD changes across the whole brain between the sad and the neutral clips ("negative movie" vs. "neutral movie" conditions), as well as during rest ("negative rest" vs. "neutral rest" conditions). These experimental conditions were modeled with 4 boxcar regressors (one per condition) in a factorial design, and subsequently used to define two different seed ROIs for connectivity analyses, one with stimulus-related activity and another with rest-related activity. While movies vs. rest recruited widespread brain areas, as expected, sad compared to neutral movies produced selective increases (P_{WFE}<.05. FWE-corrected at cluster level) predominantly in the left insula cortex (including both posterior and anterior parts, with peak MNI: -40, 4, 10; 121 voxels), together with the bilateral anterior cingulate cortex, bilateral middle frontal gyrus, and right temporal pole. As the insula has been consistently associated to emotional processing across many paradigms (34–38), most often in relation to negative valence (39), this region was selected as our first ROI (stimulus-related). Conversely, rest vs. movies activated widespread areas associated with the DMN, including medial frontal and parietal cortices, among which some were further increased during the "negative rest" than the "neutral rest" condition (P_{WFE}<.05), predominantly in bilateral precuneus (peak MNI: 4, -54, 42; 541 voxels) and to a lesser degree in occipital cortex and left medial superior frontal gyrus. This

accords with previous work reporting a modulation of the precuneus and other DMN regions at rest by preceding emotional or cognitive stimulation (40–43). We therefore selected the precuneus as the second seed (rest-related) for our subsequent connectivity analysis.

Dynamic functional connectivity analysis (CAPs identification)

To examine changes in IFNs as a function of experimental conditions (neutral movie, neutral rest, negative movie, and negative rest), we implemented a co-activation pattern (CAP) methodology (28, 44, 45). It has been previously shown (28, 46) how transient associations between fMRI signals captured by specific co-activation patterns (CAPs), correspond to the intrinsic neural architecture configured for supporting specialized functions (IFNs). Remarkably, the CAP approach provides a measure of dynamic functional connectivity with a relevant seed by decomposing fluctuations of the fMRI BOLD signals into multiple spatial patterns that reflect the instantaneous organization and reorganization of networks co-activated with the seed over time (27, 44). The two emotion-responsive ROIs identified by our GLM analysis (insula and precuneus from “negative movie” and “negative rest” conditions, respectively) were used as seeds for the CAPs generation. By using seeds defined by an independent GLM-based analysis, we could ensure to “anchor” the observed CAPs to functionally relevant networks in the current experimental paradigm, rather than highlight other less specific IFNs. Unlike static connectivity analysis based on correlations by averaging over long periods, the dFC approach with CAPs accounts for the BOLD temporal variability by representing instantaneous brain configurations at single time points (fMRI volumes) and then sorting them in a few dominant patterns through clustering analysis (27). CAPs were computed with the “tbCAPs” toolbox (47), following a stepwise pipeline illustrated in Fig. S1. A more detailed description of our methodological procedure is provided elsewhere (47). Importantly, this approach yields a temporal metric to quantify dFC variability over time by computing the occurrences of each CAP in each condition. Occurrences are defined as the sum of frames (time-points) assigned to a given CAP among all the retained frames, across the entire scanning duration.

Following the generation of CAPs for each seed, we compared their expression across the affective contexts with generalized linear mixed models [gLMMs (48)] using the R software. We performed a 2x2 gLMM-based factorial analysis comprising two fixed factors denoted by the following R-based formula syntax:

occurrences ~ context * period + (1 | subject),

where the fixed factor "context" comprised two levels corresponding to the affective valence of movies (i.e., negative or neutral) and the second factor "period" represented the type of condition (movie or rest). Individual participants (subject) were modeled as a random factor, and "occurrences" was the dependent variable, computed for each experimental condition and each CAP. This 2x2 analysis allowed us to evaluate separately the main effects of stimulus exposure (movie vs. rest) and emotional valence (negative vs. neutral), as well as their interactions, for each of the CAPs. Subsequently, only the significant CAPs showing either main effects or interactions of the factors "context" (neutral, negative) and period (movie, rest), were considered as experimentally relevant and selected for more detailed evaluation (see next section).

We also tested whether differences in the temporal metrics of these relevant CAPs were associated with behavioral measures of subjective emotional state (PANAS), using generalized estimated equations (GEEs) (49). In these analyses, the CAPs occurrences were introduced as multiple outcomes, and affective indices (PANAS scores) were the predictor variables. P values were adjusted false discovery rate (FDR) for multiple testing under dependency (50, 51).

CAPs interaction analysis

Within-CAPs interactions

To address the main goal of our study concerning functional relationships between networks in different affective states, we examined how changes in the expression of a given network correlated with changes in other networks across successive periods (e.g., movies vs. post-movie rest). First, we computed a set of within-CAP pair-wise Pearson coefficients (r) to assess the occurrence of each affectively-relevant CAP across different conditions. This analysis thus probed for context-dependent "movie-rest" transitions where occurrences during the "movie" period were correlated with occurrences during the subsequent "rest" period of the same CAP in the same affective valence [e.g., $r(DMN_{neutral\ movie}, DMN_{neutral\ rest})$; $r(DMN_{negative\ movie}, DMN_{negative\ rest})$]. As a control comparison, these within-CAP relationships were compared to movie-rest correlations between different contexts, when movies and rest conditions did not follow in direct succession [e.g., $r(DMN_{negative\ movie}, DMN_{neutral\ rest})$; $r(DMN_{neutral\ movie}, DMN_{negative\ rest})$]. Because only reporting differences in significance for different conditions [e.g., one correlation significant ($p<0.05$) for transitions in one context but not the other ($p>0.05$)] would lead to statistical fallacy (52), we could thus directly assess differences in the magnitude of context/valence-specific correlations relative to non-specific control correlations by comparing the confidence intervals (CI) of their Pearson coefficients, which allows considering both the magnitude and precision of the estimated effects (53). All within-CAP comparisons were implemented with the R-based Cocor package (54). Dependency of within-CAP correlations were considered and corrected following

Zuo et al., (53), when their comparisons included overlapping variables [e.g., r($DMN_{neutral\ movie}$, $DMN_{neutral\ rest}$) vs. r($DMN_{neutral\ movie}$, $DMN_{negative\ rest}$)].

Context-dependent between-CAPs interactions

A second set of analyses concerned the between-CAPs of interest associations, and allowed us to examine their reciprocal relationships as a function of emotional context. The correlation between occurrences of different CAPs was again computed context-wise, to probe how expression of one CAP during the movie watching period was associated to the expression of other CAPs in the just following resting state period [e.g. r($FPCN_{neutral}$, $DMN_{post\ neutral}$)]. The correlations for each pair of CAPs were then compared between the two affective contexts [e.g. r($FPCN_{neutral}$, $DMN_{post\ neutral}$) vs. r($FPCN_{negative}$, $DMN_{post\ negative}$)]. Dependency of non-overlapping variables was considered and corrected for these between-CAPs comparisons as appropriate (53). Further description of statistical tests including R-based mathematical formulae for both within-CAPs and between-CAPs comparisons are described in SI (section “Tests for comparing CAPs correlations”).

Results

Behavioral indices of emotional induction by movies

We first verified that movies with negative content induced distinctive patterns in both behavior and brain measures, compared to neutral movies. Affective ratings of movie clips confirmed a reliable difference in emotional experience with more negative valence and higher arousal elicited by the negative compared to neutral movies (Fig. 1B). PANAS scores assessing subjective affect also differed between the pre- and post-context measures as a function of emotional condition, with significant increases in the negative affect (NA) scores following negatively-valenced movies (Fig. 3A). Further behavioral results concerning the movies are described in SI (section “Psychological indices of emotion elicitation”).

CAPs expressed across stimulation periods and affective contexts

Two CAP analyses were conducted using the seed ROIs identified by our preliminary GLM analysis (see “Methods” section and Fig. S1A), one reflecting functional coupling with the left insula and another reflecting coupling with the precuneus. In total 14 CAPs were identified, based on a data-driven “consensus” procedure (55) indicating K=7 for each seed as the optimal number of distinct brain maps in terms of replicability for our dataset (see pipeline in Fig. S1). The spatial configuration of these CAPs is depicted in SI (Fig. S2.2) and globally accords with previous work on IFNs (2, 56–58).

Changes in temporal dynamics of CAPs across conditions

Critically, we then compared the temporal occurrences of all the 14 CAP between experimental conditions. Using a 2 (affective context) x 2 (stimulation period) factorial analysis of CAP occurrences, we found that only four out of these 14 networks were differentially expressed across the affective contexts (i.e., negative vs. neutral. Fig. S2), including the insula-connected CAP5 (in-FCPN) and the precuneus-connected CAP1, CAP3, and CAP5 (pr-VIS, pr-DMN, and pr-CEN, respectively). Peak coordinates for these four networks are listed in SI (Table S1). Below we describe each of these CAPs in turn.

Among networks co-activated with the insula, in-CAP5 was the only one showing a significant modulation by affective valence. It comprised a large set of frontoparietal regions associated with cognitive control and salience detection (5, 56), and, therefore, considered to overlap with the FPCN reported in other studies (Fig. 2A). This CAP exhibited an interaction between "affective context" and "stimulation period" [gLMM interaction: $F(54)= 4.5$; $P_{FDR} <.05$; Table S2], indicating more frequent occurrences of this network during negative movies compared to other conditions, in addition to main effects of both period [gLMM main effect "period": $F(54)= 46.6$; $P_{FDR} <.0001$. $\beta_{movie}= 19.30$, 95% CI (16.32; 22.30)], and context [gLMM main effect "context": $F(54)= 15.8$; $P_{FDR} <.001$. $\beta_{negative}= 16.83$, 95% CI (13.86; 19.80). Remarkably, 48% of the occurrences of this in-FPCN CAP across all the conditions were seen in the "negative movie" condition (in contrast to 24% during "neutral movie").

The three other emotion-sensitive CAPs were derived from the precuneus-based analysis. Most notably, the pr-CAP3 showed a very similar spatial configuration to DMN (2), encompassing medial prefrontal, posterior cingulate, and inferior parietal cortices (Fig. 2C). The factorial analysis indicated a main effect of "affective context" [gLMM main effect "context": $F(54)= 4.9$; $P_{FDR} <.05$; $\beta_{negative}= 16.7$, 95% CI (13.85; 19.60)], but there was no significant effect of stimulation period [gLMM main effect "period": $F(54) = 2.2$; $P_{FDR} <.1$; $\beta_{rest}= 16.74$, 95% CI (13.18; 19.01)], nor any "context" x "period" interaction [gLMM interaction: $F(54)= 0.27$; $P_{FDR} <1$; see Table S2]. However, this DMN CAP dominated in the "negative rest" condition", which represented 32% of its occurrences across conditions (vs. 22% during neutral rest). In contrast, the pr-CAP5 involved dorso-lateral fronto-parietal areas (Fig. 2D) commonly associated with the central executive network (CEN) (58, 59). This network also showed a significant interaction between "affective context" and "stimulation period" [gLMM interaction: $F(54)= 10.2$; $P_{FDR}< .001$; see Table S2], elicited by a combination of increased occurrences in the "neutral" conditions [gLMM main effect "context": $F(54)= 4.5$; $P_{FDR} < .001$. $\beta_{neutral}= 15.58$, 95% CI (12.45; 18.70)] and in the "movie" conditions [gLMM main effect "period": $F(54) = 7.0$; $P_{FDR} <.0001$; $\beta_{movie}= 16.11$, 95% CI (12.98;

19.20)]. Thus, unlike the pr-DMN_{CAP3}, the pr-CEN_{CAP5} showed the highest number of occurrences during the "neutral movie" condition (39% of its total occurrence vs. 21% during negative movies).

Finally, the pr-CAP1 overlapped with a classic "visual network" centered on occipital and posterior parietal areas (VIS, Fig. 2B) (60–66). It showed a distinctive increase of occurrence rates during the "negative movie" condition, with main effects of both "affective context" [gLMM main effect "context": $F(54) = 7.9$; $P_{FDR} < .01$. $\beta_{negative} = 18.40$, 95% CI (15.94; 20.90)] and "stimulation period" [gLMM main effect "period": $F(54) = 4.4$; $P_{FDR} < 0.05$. $\beta_{movie} = 17.79$, 95% CI (15.33; 20.30)], reflecting generally higher occurrences during movies than rest and during negative than neutral conditions, respectively. However, there was no significant "period" x "context" interaction [gLMM interaction: $F(54) = 2.1$; $P_{FDR} < .1$. Table S2] despite its predominance during the negative movies, in which the pr-VIS exhibited 35% of total occurrences across conditions (vs. 21% during neutral movies).

Altogether, these data converge with previous studies to indicate that emotional events produce distinctive and coordinated effects on specific IFNs, especially the DMN and higher regulatory systems associated with FPCN and CEN, with significant carry-over effects lingering beyond emotional events themselves and extending into subsequent rest periods.

Relationship of brain CAPs with behavioral measures of affect

To probe for the behavioral significance of changes observed in brain networks across conditions, we examined whether the individual occurrences of each relevant CAP could predict subjective affective rating scores (from PANAS) that were obtained at the end of scanning runs in each emotional context. Results from our GEE analysis showed that more negative affect (NA) scores post-scanning were associated with higher occurrences of in-FPCN CAP during the "negative movie" period ($\beta = .24$, 95% CI (0.15;0.33); $P_{FDR} < 01$; Fig. 3B. Up-right), and inversely to lower occurrences of in-FPCN during the "negative rest" period ($\beta = -.32$, 95% CI (-0.30; 0.13); $P_{FDR} <$ 05, Fig. 3B. Bottom-right). On the other hand, occurrences of the pr-DMN CAP during the same "negative rest" condition also showed a positive correlation with the post-scanning NA scores ($\beta =$ .20, 95% CI (0.20; 0.46), $P_{FDR} < 01$). Fig 3B. Bottom-right). Thus, higher NA scores following exposure to the "negative context" were linked not only to greater occurrences of in-FPCN during negative movies, but also to lesser occurrences of in-FPCN accompanied with greater occurrences of pr-DMN during the subsequent "negative rest" period. By contrast, positive affect (PA) scores were not related to the expression of any of these networks (see Fig. 3. Left).

Functional interactions within CAPs.

Finally, we turned to the key question of our study. Namely, whether the reciprocal relationships between brain networks *during* and *after* movie episodes were modified by their affective valence (i.e., neutral or negative). To do so, we first computed movie-rest correlations in individual occurrences for each CAP of interest (pr-VIS, pr-DMN, pr-CEN, and in-FPCN) across all participants, and then examined how these relationships differed between the two affective contexts [within-CAP transitions; e.g., $r(CAP(i)_{neutral\ movie}; CAP(i)_{neutral\ rest})$ vs. $r(CAP(i)_{negative\ movie}; CAP(i)_{negative\ rest})$]. Remarkably, we observed a consistent anticorrelation between the expression of a given CAP during movie periods and its expression during subsequent rest, for both affective contexts and for the pr-VIS, pr-DMN, and in-FPCN CAPs, but not for pr-CEN (see Fig. 5A). Although these anticorrelations were numerically higher in the negative context (r values -.46 to -.67) than the neutral context (-.33 to -.39), a direct comparison of anticorrelation magnitudes (see methods) showed no significant difference for any of the four CAPs.

However, the within-CAP correlations for transitions from movie to rest conditions were significantly modulated by affective context in comparison to control conditions when the movies and rest did not follow in direct succession [e.g., $r(CAP(i)_{neutral\ movie}; CAP(i)_{negative\ rest}]$, but selectively for the pr-DMN (Fig. 4) and not for the three other networks. Thus, for the pr-DMN CAP, the anticorrelation pattern observed during the post "negative movie" transition to the subsequent "negative rest" condition across all participants [$r(19)=-.67$; $P_{FDR}<.01$] was significantly higher relative to the anticorrelation between non-successive "negative movie" and "neutral rest" periods [$r(19)=-.19$; $P_{FDR}< 1$. $P_{corrected}<.05$, CI=(-1.16; -.03) for the difference], or relative to the anticorrelation observed between non-successive neutral movie and negative rest periods [$r(19)=-.05$; $P_{FDR}<1$. $P_{corrected}<.05$, CI=(-1.14 -.04) for the difference]. None of the other CAPs showed any difference in these comparisons (Table S3).

Altogether, these data highlight robust antagonistic relationships between the expression of particular functional networks during active movie watching and their subsequent expression during rest, regardless of affective state (except for the pr-CEN CAP), but with a distinctive impact of negative emotion on these transitions for the pr-DMN CAP (Fig.4).

Functional interactions between CAPs

Lastly, we examined reciprocal interactions among networks by determining whether the occurrence rate of a given CAP of interest during movie watching could predict the occurrence of *other* CAPs during the following rest period, and tested whether this relationship varied in a

context-dependent manner for negative compared to neutral conditions (between-CAP analysis; e.g. r(CAP(i)$_{\text{negative movie}}$; CAP(j)$_{\text{negative rest}}$) vs. r(CAP(i)$_{\text{neutral movie}}$; CAP(j)$_{\text{neutral rest}}$)]. Results from this analysis (Fig. 5B) revealed a positive association between the in-FPCN in the movie-watching period and pr-CEN in subsequent resting period in the "neutral" context [r(19)= .54; P_{FDR}<.05], which was significantly different [$P_{corrected}$ <.05; CI=(-0.02; -.03). Fig. 5B.] from the suppression of such interaction in the "negative" context [r(19)=.-19; P_{FDR}<1]. Conversely, the in-FPCN during movie watching exhibited a positive correlation with the pr-DMN during subsequent rest exclusively in the "negative" context [r(19)=.28; P_{FDR} <1], absent in the "neutral" context [r(19)=-.34; P_{FDR}<1], with a significant difference between the two contexts [$P_{corrected}$ <.05; CI=(-1.17; 0.10). Fig. 5B]. On the other hand, the pr-DMN during movie watching was strongly anticorrelated with the pr-CEN during subsequent rest exclusively in the "negative" context [r(19)=.-61; P_{FDR}<.01], a significant difference [$P_{corrected}$<.05; CI=(0.02; 1.20)] compared to the absence of such correlation in the neutral context [r(19)=-.11; P_{FDR}<1] (Fig. 5B). Other relationships between pairs of networks were not significant and not modulated by affective context.

Discussion

Our study identified a set of distributed brain networks with dynamically fluctuating co-activation patterns (27, 44, 47) that were modulated by negative emotion, with differential expression (i.e., occurrences) and interactions (i.e., correlations) observed both during emotional stimulation itself (sad movies) and during its aftermath (subsequent rest). Specifically, we uncovered four networks whose temporal profile differed as a function of emotional conditions, overlapping with the DMN, CEN, FPCN, and VIS networks reported in other studies. These results show, first, that negative emotional events engage a select set of brain-wide systems, with anatomically and temporally specific connectivity arising not only during emotional events, but also extending during subsequent rest (Fig.2). Second, the occurrences of some of these CAPs is directly related to subjective emotional state, with more negative affect (NA) reported by participants who show more frequent occurrences of FPCN and DMN during and after negative movies, respectively (Fig.3). Third, we observed specific temporal relationships "within" and "between" these networks, such that their expression rate during movie periods predicted their expression in subsequent rest. Critically, these functional dynamics among networks differed significantly in the negative affective compared to the neutral conditions (Figs. 4-5). Together, these data provide new evidence on how brain-wide systems are dynamically and interactively recruited by emotions and their regulation, with robust carry-over effects beyond emotional events themselves. These neural results add to behavioral evidence of "emotional inertia" (23, 67) and suggest that emotion regulation processes may extend over protracted periods of time following emotion elicitation.

More generally, our study provides new insights on affective brain dynamics and uncovers useful neural markers for adaptive regulation mechanisms that mediate a restoration of homeostatic balance after stressful events, possibly altered in psychopathological conditions such as depression, anxiety, or PTSD.

Emotion-responsive CAPs with different temporal profiles and different functional roles

Among networks differentially modulated by negative emotion, the pr-VIS CAP comprised visual areas (68) mainly located in dorsal extrastriate cortex and mostly engaged during the "negative movie" periods. This accords with abundant evidence for enhanced activity of the visual system in response to affective stimulation (57, 69), presumably reflecting modulatory top-down signals from emotion-responsive limbic areas (70, 71). Nevertheless, pr-VIS activity showed no direct interaction with the expression of other CAPs of interest, consistent with these sensory areas having no direct link with emotional experience per se. On the other hand, the in-FPCN CAP also predominated during emotion elicitation periods (negative movie), but its occurrences correlated with negative affect scores reported after scanning. Anatomically, in-FPCN comprised components of the "salience" and "dorsal attention" systems, typically engaged in the appraisal of arousing information (72). This pattern fits well with theoretical accounts (73, 74) according to which emotion involves an integration of processes associated with selective attention (75), interoception (38), and detection of behavioral relevance (76). Higher in-FPCN expression during the negative movie indicates this network is an important component of neural processes underlying emotion elicitation (72, 77).

In contrast, the pr-DMN-CAP showed the greatest number of occurrences during rest periods following negative movies, and its presence also correlated with negative affect scores. These results add to recent findings of similar aftermaths of emotionally arousing stimuli during resting state, e.g., following fearful or joyful movies (20) as well as reward or punishment outcomes (22, 78). Emotional carry-over effects in brain connectivity may also underpin changes in affective and cognitive responses to future events (79), and thus contribute to adaptive behavioral functions of emotions. Enhanced pr-DMN activity at rest has previously been associated with self-referential mental activity and introspection (2, 41), autobiographical memory (80), as well as mood disorders (81–83). Pr-DMN upregulation is often regarded as a biomarker for depressive rumination (84–86), possibly resulting from emotion dysregulation (87). Moreover, both spontaneous emotion regulation strategies (88, 89) and voluntary cognitive reappraisal (90, 91) enhance DMN connectivity, suggesting a link with functional recovery mechanisms acting to downregulate negative emotions as observed in the post sad movie rest periods here.

Additionally, in our study, pr-DMN was the only CAP exhibiting a significant impact of the negative affective context on functional transitions between its expression rate during rest and its expression during the just preceding movie (within-CAP dynamics). Although a consistent anticorrelation of CAP occurrences between movie and rest periods (i.e., more frequent occurrences during movies predicting less frequent occurrences during rest) was observed for all emotion-responsive networks (except pr-CEN), only the pr-DMN showed a statistically significant amplification of this antagonistic relationship for negative rest periods that directly followed negative movie periods. In other words, the lower the expression of DMN during the sad movie, the higher its expression during subsequent aftermath at rest (see Fig. 4). This strong and valence-dependent shift in dFC provides new evidence for a key role of the DMN in homeostatic adjustment after acute stressors (26), possibly through coordinated interactions with other brain networks (see below). Nevertheless, it remains to fully determine the factors accounting for such "push-pull" DMN anticorrelations in occurrences between emotional episodes and subsequent recovery periods at rest. Importantly, the absence of such behavior in movie-rest transitions for the pr-CEN indicates that this functional shift in connectivity state is not caused by non-specific rebound or hemodynamic effects but appear both network-specific and context-sensitive.

Finally, the pr-CEN showed a distinctive profile in occurrences, with predominant expression during neutral movies relative to other conditions. This CAP comprised dorsal ACC and dorsolateral prefrontal areas associated with effortful executive control (92), presumably activated by more abstract cognitive demands to process the content of neutral movies (unlike more natural absorption by emotional scenes). Nevertheless, the pr-CEN exhibited significant changes in its interaction with other CAPs as a function of affective context, as demonstrated by our analysis of between-CAPs relationship and discussed below.

Emotion-related modulation of functional interactions between CAPs

A key finding of our study is that higher or lower expression of certain CAPs during the movie period was associated with different occurrences of *other* CAPs during the subsequent rest period (between-CAPs temporal dynamics), and these relationships among networks were significantly modified by the emotional context. Most critically, negative emotion produced a significant shift in the functional impact of in-FPCN activity on subsequent pr-DMN and pr-CEN at rest, such that a strong relationship of in-FPCN with pr-CEN in the neutral context was suppressed in the negative context, and replaced by a positive relationship with pr-DMN instead (Fig. 5B). Thus, higher occurrences of in-FPCN during sad movies (which correlated with more negative affect) predicted greater presence of the pr-DMN at rest following these movies (which also correlated with negative affect). This suggests that higher affective salience encoded by in-FPCN might enhance subsequent self-regulatory processes and ruminative thoughts subserved

by pr-DMN (93). We note that the magnitude of correlations between in-FPCN and subsequent pr-DMN activity was numerically modest in both affective contexts but shifted from a negative relationship in the neutral context (r= -.34) to a positive relationship in the negative context (r=.28), a highly significant difference between these two conditions.

In parallel, pr-CEN expression at rest also shifted from a strong positive correlation with in-FPCN occurrences during the preceding movie in the neutral context, to a strong negative correlation with pr-DMN occurrences in the negative context, both representing highly significant changes in correlation magnitude and/or direction. These opposing effects on pr-CEN may accord with behavioral evidence for impaired executive control abilities after acute stress conditions (94), which could be mediated at least partly by inhibitory interactions from pr-DMN in the post-negative context. Conversely, the positive relationship between in-FPCN and subsequent pr-CEN at rest in the neutral context suggests more synergic interactions between these two networks, commonly implicated in externally oriented cognition (95, 96). Interestingly, such modulation of pr-CEN expression by preceding movie valence, despite low occurrences of pr-CEN at rest overall (Fig. 2D), underscores that a high occurrence rate is not a prerequisite for measuring significant changes in CAP dynamics, and further shows that emotion may impact on the functional integration of brain networks rather than just their global activation level (11).

In sum, our findings show not only distinctive patterns of expression of in-FPCN and pr-DMN CAPs during negative emotion episodes and post-emotion rest periods, respectively, but also significant functional relationships between these networks during the transition from emotion episodes to subsequent rest. Together, these data point to complementary roles of FPCN in the integration of emotion elicitation processes and of DMN in self-regulation mechanisms contributing to affective homeostasis.

Outstanding issues and further directions

Although we found robust differences in the expression and correlation of relevant CAPs in our study, and carefully counterbalanced conditions between participants, we cannot fully rule out that other effects related to movie contents or time contributed to changes in network activity and their functional relationships as observed here. Further research using other naturalistic designs and evoking different emotions (e.g., frustration, joy, etc.) will also be valuable to confirm and extend our results. In addition, our gender selection was limited to female participants, based on pilot data showing higher and more consistent emotion ratings than males, and previous studies showing more intense emotion experiences in females (97). It will be important to replicate and extend the current findings to male populations, because emotion dysregulation and resilience to stress may show important gender differences.

Conclusions

Using a recent dFC analysis methodology (CAPs), we shed new light on the spatio-temporal organization of brain networks underlying the dynamics of negative affective experience and subsequent return to rest. Our data unveil specific transitions in the connectivity and reciprocal relationship of brain-wide networks involved in visual perception, attention to salient stimuli, executive control, and introspective self-monitoring processes during both emotional episodes (movies) and their aftermath (subsequent rest). Among these networks, the in-FCPN and pr-DMN CAPs were found to play a pivotal role in the temporal dynamics of emotional experience, from elicitation to subsequent recovery, entertaining reciprocal relationships not only with each other but also with the pr-CEN CAP. Crucially, individual occurrences of these CAPs during movies and rest were directly linked to the subjective affective state reported by participants. These findings provide novel insights on brain mechanisms underlying emotion experience and regulation (64, 98, 99), resilience to stress (100), and perseverative ruminative thinking in negative mood states (14, 20, 101). In turn, they may also offer valuable biomarkers for understanding and assessing the neural basis of clinical psychopathology conditions.

Acknowledgments

This work was supported by the Swiss excellence Scholarship program, the Schmidheiny foundation, and the Colombian Science Ministry (JG), as well as by a Sinergia Grant no. 180319 from the Swiss National Science Foundation (SNF), by the Swiss Center of Affective Sciences financed by UNIGE and SNF (Grant no. 51NF40_104897), and by the Société Académique de Genève (SACAD). This study was conducted on the imaging platform at the Brain and Behavior Lab (BBL) and benefited from support of the BBL technical staff. Imaging analysis was carried out at University of Geneva on the high-performance computing (HPC) BAOBAB server. Derived data supporting the findings of this study are available from the corresponding author [JG] on request.

Figures

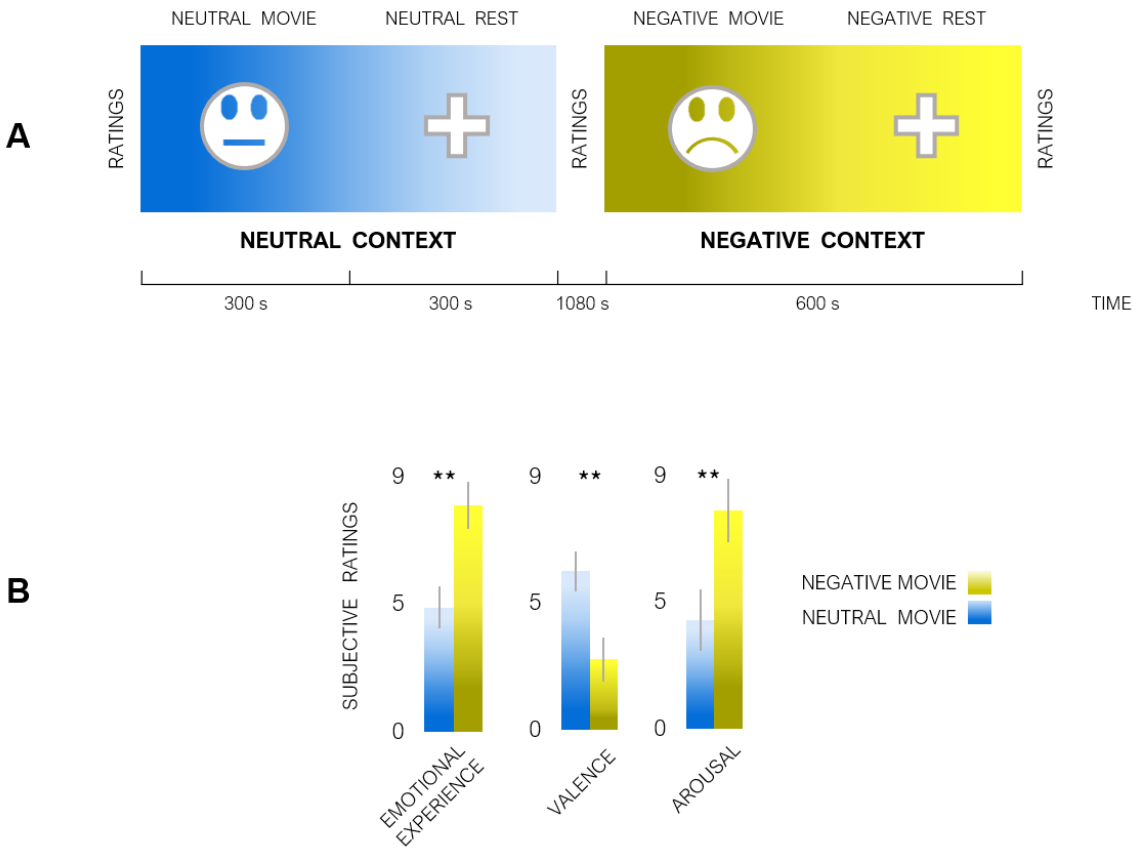

Figure 1. Behavioral paradigm. A) Paradigm design illustrating the sequence of experimental events. Negatively-valenced or neutral movies were followed by a resting period. The presentation of the two affective contexts (i.e., "neutral" and "negative") was counterbalanced across participants. **B)** Subjective affective ratings of movies obtained after each experimental context. Whiskers stand for standard errors of means. P_{FDR} adjustment for multiple comparisons (** p<.01).

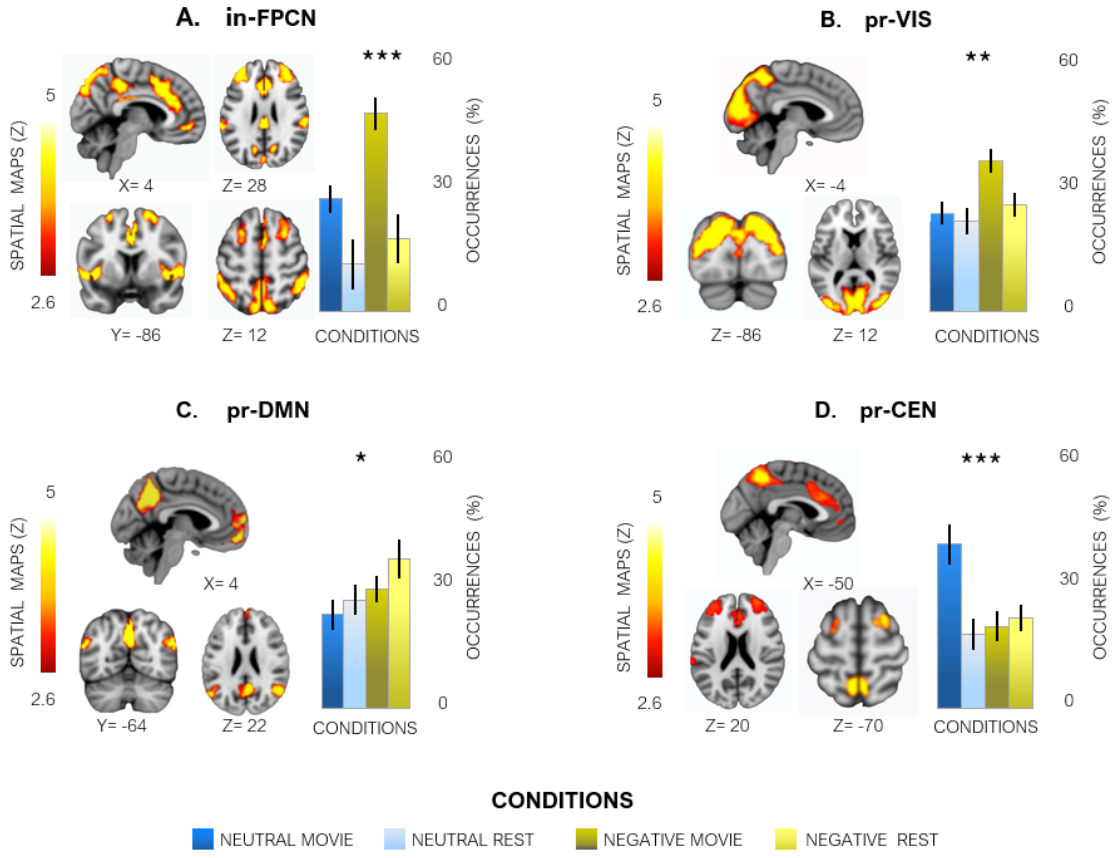

Figure 2. Spatiotemporal CAPs modulated by affective context. Functional brain networks were identified using co-activation pattern analysis (CAP) based on time-dependent coupling with the insula [A. FPCN (frontoparietal control network)] or with the precuneus [B. VIS(visual network), C. DMN (default mode network), D. CEN (central executive network)]. Only these four CAPs showed a signifcant modulation of their occurrence rate as a function of experimental condition (see suppl. Fig. S2). The brain topography maps of each CAP is illustrated with a threshold of z > 2.58 (equivalent to p<.01). Further anatomical information on peak regions is provided in Table S1. Temporal occurrence rates are plotted to show their expression (%) across experimental conditions. Statistical assesments of CAPs variance and interactions are reported in Table S2., and Fig. S2. P_{FDR} adjustment for multiple comparisons (* p<.05; ** p<.01; ***p<.001).

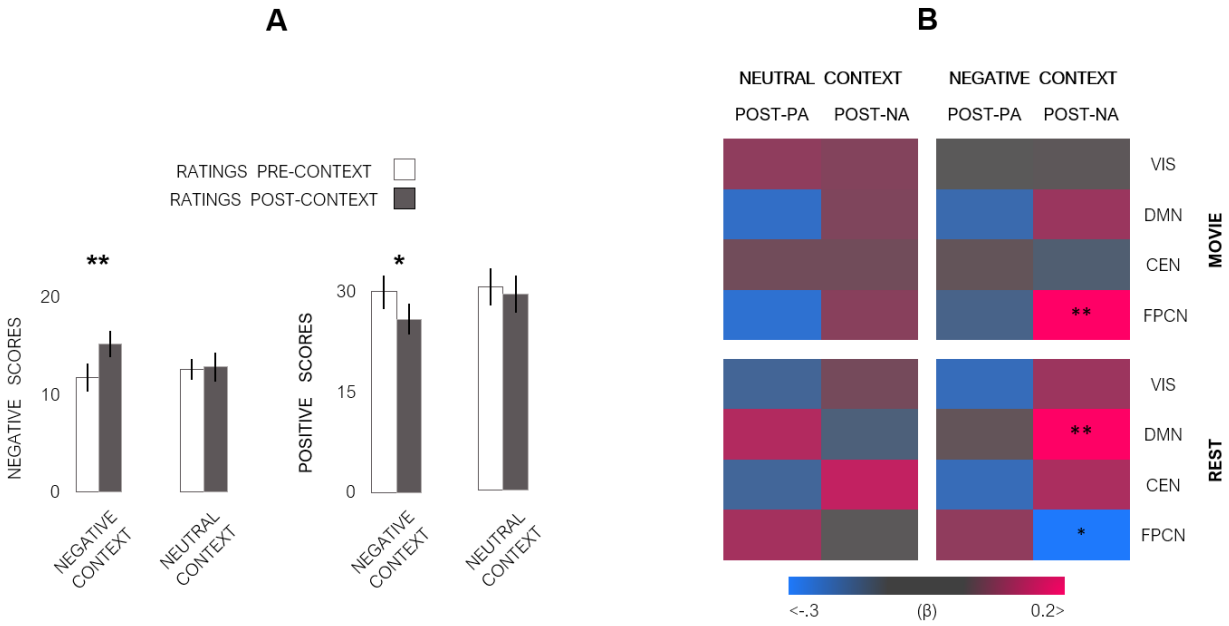

Figure 3. PANAS scores and their associations with CAPs across conditions. A) Mean scores on PANAS self-reports obtained before (pre) and after (post) each of the experimental contexts (neutral and negative). **B)** Beta (β) values of GEE-based associations between affective scores [positive (PA) and negative (NA)] and occurrence rates of the CAPs of interest. FPCN occurrences observed during the "negative movie", as well as FPCN and DMN occurrences during the "negative rest" conditions were significantly correlated with the negative affect scores (NA) measured at the end (post) of the negative context. P_{FDR} adjustment for multiple comparisons (* p<.05; ** p<.01).

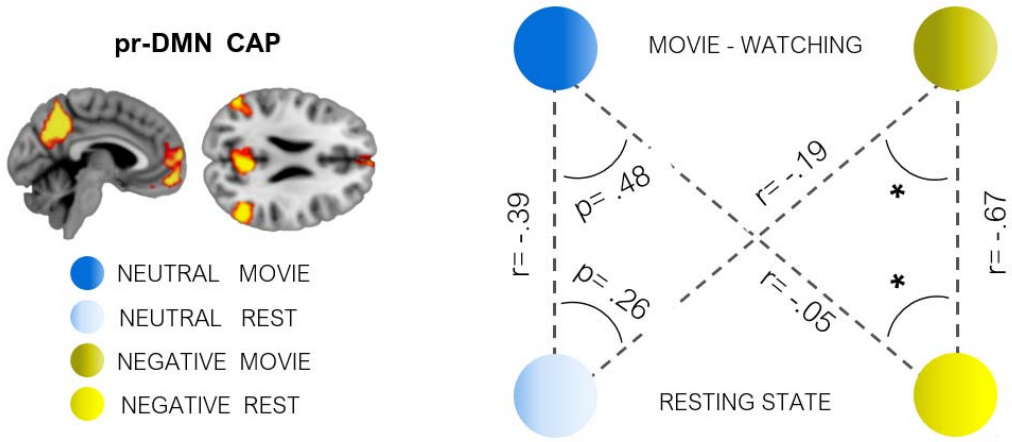

Figure 4. Within-DMN CAP interactions across . Comparisons of the movie-rest anticorrelation for the DMN (temporal occurrences per condition), illustrating significant differences for transitions between successive movie-rest periods in the negative context (yellow colors), relative to control comparisons with conditions from the "neutral" context (blue colors). The other three CAPs of interest (VIS,CEN, FPCN) showed no such effect of negative emotion on the same transitions. * p<.05. Multiple significance testing and dependency of correlations across conditions was considered and corrected when comparisons included overlapping variables (see methods).

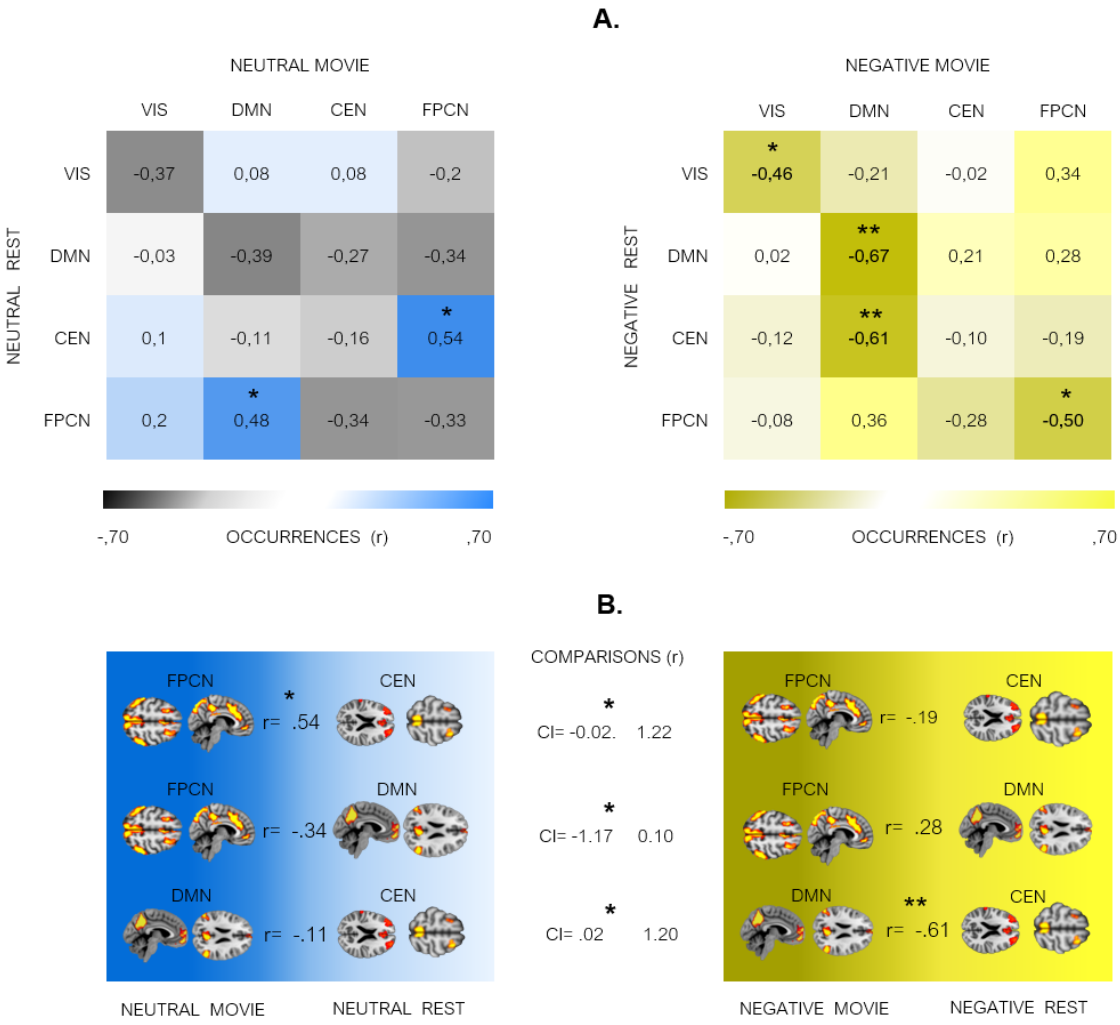

Figure 5. Between-CAPs interactions across time. A. Pairwise correlations in occurrences between CAPs of interest observed during movies and rest periods, respectively, computed for the "neutral" (left) and the "negative" context (right), P_{FDR} adjustment for multiple comparisons (* p<0.05; ** p<0.01). **B.** Comparisons of between-CAPs correlations that showed significant differences between the two emotion contexts. Multiple significance testing and dependency of non-overlapping variables were considered and corrected (see methods).

References

1. M. D. Fox, *et al.*, The human brain is intrinsically organized into dynamic, anticorrelated functional networks. *Proc. Natl. Acad. Sci.* 102, 9673–9678 (2005).

2. K. Christoff, Z. C. Irving, K. C. R. Fox, R. N. Spreng, J. R. Andrews-Hanna, Mind-wandering as spontaneous thought: a dynamic framework. *Nat. Rev. Neurosci.* 17, 718–731 (2016).

3. D. A. Fair, *et al.*, The maturing architecture of the brain's default network. *Proc. Natl. Acad. Sci.* 105, 4028–4032 (2008).

4. R. N. Spreng, R. A. Mar, A. S. N. Kim, The Common Neural Basis of Autobiographical Memory, Prospection, Navigation, Theory of Mind, and the Default Mode: A Quantitative Meta-analysis. *J. Cogn. Neurosci.* 21, 489–510 (2009).

5. M. L. Dixon, *et al.*, Heterogeneity within the frontoparietal control network and its relationship to the default and dorsal attention networks. *Proc. Natl. Acad. Sci.* 115, E1598–E1607 (2018).

6. M. L. Dixon, *et al.*, Interactions between the default network and dorsal attention network vary across default subsystems, time, and cognitive states. *Neuroimage* 147, 632–649 (2017).

7. L. Nummenmaa, *et al.*, Emotions promote social interaction by synchronizing brain activity across individuals. *Proc. Natl. Acad. Sci.* 109, 9599–9604 (2012).

8. J. Gaviria, *et al.*, Brain functional connectivity dynamics at rest in the aftermath of affective and cognitive challenges. *Hum. Brain Mapp.*, hbm.25277 (2020).

9. K. R. Scherer, Emotions are emergent processes: They require a dynamic computational architecture. *Philos. Trans. R. Soc. B Biol. Sci.* 364, 3459–3474 (2009).

10. B. Meuleman, D. Rudrauf, Induction and profiling of strong multi-componential emotions in virtual reality. *IEEE Trans. Affect. Comput.*, 1–15 (2018).

11. J. Leitão, B. Meuleman, D. Van De Ville, P. Vuilleumier, *Computational imaging during video game playing shows dynamic synchronization of cortical and subcortical networks of emotions* (2020).

12. R. L. Buckner, L. M. DiNicola, The brain's default network: updated anatomy, physiology and evolving insights. *Nat. Rev. Neurosci.* (2019) https:/doi.org/10.1038/s41583-019-0212-7.

13. R. H. Kaiser, J. R. Andrews-Hanna, T. D. Wager, D. A. Pizzagalli, Large-scale network dysfunction in major depressive disorder: A meta-analysis of resting-state functional connectivity. *JAMA Psychiatry* 72, 603–611 (2015).

14. B. J. Harrison, *et al.*, Modulation of Brain Resting-State Networks by Sad Mood Induction. *PLoS One* 3, e1794 (2008).

15. V. Borchardt, *et al.*, Echoes of Affective Stimulation in Brain connectivity Networks. *Cereb. Cortex* 28, 4365–4378 (2018).

16. N. Zovetti, *et al.*, Default mode network activity in bipolar disorder. *Epidemiol. Psychiatr. Sci.* 29, e166 (2020).

17. G. Rey, *et al.*, Modulation of brain response to emotional conflict as a function of current mood in bipolar disorder: Preliminary findings from a follow-up state-based fMRI study.

Psychiatry Res. - Neuroimaging 223, 84–93 (2014).

18. W. Zhang, *et al.*, Acute stress alters the 'default' brain processing. *Neuroimage* (2019) https:/doi.org/10.1016/j.neuroimage.2019.01.063.

19. A. Barnes, E. T. Bullmore, J. Suckling, Endogenous Human Brain Dynamics Recover Slowly Following Cognitive Effort. *PLoS One* 4, e6626 (2009).

20. H. Eryilmaz, D. Van De Ville, S. Schwartz, P. Vuilleumier, Impact of transient emotions on functional connectivity during subsequent resting state: A wavelet correlation approach. *Neuroimage* 54, 2481–2491 (2011).

21. H. J. F. van Marle, E. J. Hermans, S. Qin, G. Fernández, Enhanced resting-state connectivity of amygdala in the immediate aftermath of acute psychological stress. *Neuroimage* 53, 348–354 (2010).

22. S. Pichon, E. A. Miendlarzewska, H. Eryilmaz, P. Vuilleumier, Cumulative activation during positive and negative events and state anxiety predicts subsequent inertia of amygdala reactivity. *Soc. Cogn. Affect. Neurosci.* 10, 180–190 (2015).

23. P. Kuppens, P. Verduyn, Emotion dynamics. *Curr. Opin. Psychol.* 17, 22–26 (2017).

24. K. Apazoglou, *et al.*, Rumination related activity in brain networks mediating attentional switching in euthymic bipolar patients. *Int. J. Bipolar Disord.* 7, 3 (2019).

25. J. P. Lamke, *et al.*, The impact of stimulus valence and emotion regulation on sustained brain activation: Task-rest switching in emotion. *PLoS One* 9 (2014).

26. E. J. Hermans, M. J. a G. Henckens, M. Joëls, G. Fernández, Dynamic adaptation of large-scale brain networks in response to acute stressors. *Trends Neurosci.* 37, 304–14 (2014).

27. X. Liu, N. Zhang, C. Chang, J. H. Duyn, Co-activation patterns in resting-state fMRI signals. *Neuroimage*, 1–10 (2018).

28. X. Liu, J. H. Duyn, Time-varying functional network information extracted from brief instances of spontaneous brain activity. *Proc. Natl. Acad. Sci.* 110, 4392–4397 (2013).

29. X. Protopopescu, *et al.*, Orbitofrontal cortex activity related to emotional processing changes across the menstrual cycle. *Proc. Natl. Acad. Sci.* 102, 16060–16065 (2005).

30. N. Petersen, L. A. Kilpatrick, A. Goharzad, L. Cahill, Oral contraceptive pill use and menstrual cycle phase are associated with altered resting state functional connectivity. *Neuroimage* 90, 24–32 (2014).

31. B. Pletzer, J. S. Crone, M. Kronbichler, H. Kerschbaum, Menstrual Cycle and Hormonal Contraceptive-Dependent Changes in Intrinsic Connectivity of Resting-State Brain Networks Correspond to Behavioral Changes Due to Hormonal Status. *Brain Connect.* 6, 572–585 (2016).

32. J. Endicott, The menstrual cycle and mood disorders. *J. Affect. Disord.* 29, 193–200 (1993).

33. J. M. Andreano, A. Touroutoglou, B. Dickerson, L. Feldman B., Hormonal Cycles, Brain Network Connectivity, and Windows of Vulnerability to Affective Disorder. *Trends Neurosci.* 41, 660–676 (2018).

34. L. H. Somerville, *et al.*, Interactions between transient and sustained neural signals support the generation and regulation of anxious emotion. *Cereb. Cortex* 23, 49–60

(2013).

35. M. P. Paulus, J. S. Feinstein, G. Castillo, A. N. Simmons, M. B. Stein, Dose-dependent decrease of activation in bilateral amygdala and insula by lorazepam during emotion processing. *Arch. Gen. Psychiatry* 62, 282–288 (2005).

36. E. Benelli, *et al.*, Emotional and cognitive processing of narratives and individual appraisal styles: Recruitment of cognitive control networks vs. modulation of deactivations. *Front. Hum. Neurosci.* 6, 1–16 (2012).

37. Y. Liu, H. Huang, M. McGinnis-Deweese, A. Keil, M. Ding, Neural substrate of the late positive potential in emotional processing. *J. Neurosci.* 32, 14563–14572 (2012).

38. H. D. Critchley, S. N. Garfinkel, Interoception and emotion. *Curr. Opin. Psychol.* 17, 7–14 (2017).

39. B. Knutson, K. Katovich, G. Suri, Inferring affect from fMRI data. *Trends Cogn. Sci.* 18, 422–428 (2014).

40. T. C. Ho, *et al.*, Emotion-dependent functional connectivity of the default mode network in adolescent depression. *Biol. Psychiatry* 78, 635–646 (2015).

41. K. C. R. Fox, *et al.*, Affective neuroscience of self-generated thought. *Ann. N. Y. Acad. Sci.* 1426, 25–51 (2018).

42. R. N. Spreng, W. D. Stevens, J. P. Chamberlain, A. W. Gilmore, D. L. Schacter, Default network activity, coupled with the frontoparietal control network, supports goal-directed cognition. *Neuroimage* 53, 303–317 (2010).

43. G. Northoff, How do resting state changes in depression translate into psychopathological symptoms? from “Spatiotemporal correspondence” to “Spatiotemporal Psychopathology.” *Curr. Opin. Psychiatry* 29, 18–24 (2016).

44. M. G. Preti, T. A. W. Bolton, D. Van De Ville, The dynamic functional connectome: State-of-the-art and perspectives. *Neuroimage* 160, 41–54 (2017).

45. C. Chang, *et al.*, Tracking brain arousal fluctuations with fMRI. *Proc. Natl. Acad. Sci. U. S. A.* 113, 4518–23 (2016).

46. X. Liu, C. Chang, J. H. Duyn, Decomposition of spontaneous brain activity into distinct fMRI co-activation patterns. *Front. Syst. Neurosci.* 7, 101 (2013).

47. T. A. W. Bolton, *et al.*, TbCAPs: A toolbox for co-activation pattern analysis. *Neuroimage* 211, 116621 (2020).

48. M. E. Brooks, *et al.*, glmmTMB Balances Speed and Flexibility Among Packages for Zero-inflated Generalized Linear Mixed Modeling. *R J.* 9, 378 (2017).

49. S. Pekár, M. Brabec, Generalized estimating equations: A pragmatic and flexible approach to the marginal GLM modelling of correlated data in the behavioural sciences. *Ethology* 124, 86–93 (2018).

50. Y. Benjamini, Y. Hochberg, Controlling the False Discovery Rate: A Practical and Powerful Approach to Multiple Testing. *J. R. Stat. Soc. Ser. B* 57, 289–300 (1995).

51. Y. Benjamini, D. Yekutieli, The control of the false discovery rate in multiple testing under dependency. *Ann. Stat.* 29, 1165–1188 (2001).

52. S. Nieuwenhuis, B. U. Forstmann, E.-J. Wagenmakers, Erroneous analyses of interactions in neuroscience: a problem of significance. *Nat. Neurosci.* 14, 1105–1109

(2011).

53. G. Y. Zou, Toward using confidence intervals to compare correlations. *Psychol. Methods* 12, 399–413 (2007).

54. B. Diedenhofen, J. Musch, Cocor: A comprehensive solution for the statistical comparison of correlations. *PLoS One* 10, 1–12 (2015).

55. S. Monti, P. Tamayo, J. Mesirov, T. Golub, Consensus clustering: A resampling-based method for class discovery and visualization of gene expression microarray data. *Mach. Learn.* 52, 91–118 (2003).

56. M. W. Cole, G. Repovš, A. Anticevic, The frontoparietal control system: A central role in mental health. *Neuroscientist* 20, 652–664 (2014).

57. P. A. Kragel, M. C. Reddan, K. S. LaBar, T. D. Wager, Emotion schemas are embedded in the human visual system. *Sci. Adv.* 5 (2019).

58. P. S. Goldman-Rakic, Architecture of the Prefrontal Cortex and the Central Executive. *Ann. N. Y. Acad. Sci.* 769, 71–84 (1995).

59. V. Menon, L. Q. Uddin, Saliency, switching, attention and control: a network model of insula function. *Brain Struct. Funct.* 214, 655–667 (2010).

60. D. Kang, Y. Liu, V. Miskovic, A. Keil, M. Ding, Large-scale functional brain connectivity during emotional engagement as revealed by beta-series correlation analysis. *Psychophysiology* 53, 1627–1638 (2016).

61. X. Liu, *et al.*, Subcortical evidence for a contribution of arousal to fMRI studies of brain activity. *Nat. Commun.* 9, 1–10 (2018).

62. D. H. O'Connor, M. M. Fukui, M. A. Pinsk, S. Kastner, Attention modulates responses in the human lateral geniculate nucleus. *Nat. Neurosci.* 5, 1203–1209 (2002).

63. H. Saarimäki, *et al.*, Distributed affective space represents multiple emotion categories across the human brain. *Soc. Cogn. Affect. Neurosci.* 13, 471–482 (2018).

64. C. Sripada, *et al.*, Volitional regulation of emotions produces distributed alterations in connectivity between visual, attention control, and default networks. *Neuroimage* 89, 110–121 (2014).

65. M. C. Riedel, *et al.*, Dissociable meta-analytic brain networks contribute to coordinated emotional processing. *Hum. Brain Mapp.* 39, 2514–2531 (2018).

66. M. Göttlich, Z. Ye, A. Rodriguez-Fornells, T. F. Münte, U. M. Krämer, Viewing socio-affective stimuli increases connectivity within an extended default mode network. *Neuroimage* 148, 8–19 (2017).

67. P. Kuppens, Z. Oravecz, F. Tuerlinckx, Feelings change: Accounting for individual differences in the temporal dynamics of affect. *J. Pers. Soc. Psychol.* 99, 1042–1060 (2010).

68. G. A. Orban, D. Van Essen, W. Vanduffel, Comparative mapping of higher visual areas in monkeys and humans. *Trends Cogn. Sci.* 8, 315–324 (2004).

69. P. Vuilleumier, M. P. Richardson, J. L. Armony, J. Driver, R. J. Dolan, Distant influences of amygdala lesion on visual cortical activation during emotional face processing. *Nat. Neurosci.* 7, 1271–1278 (2004).

70. P. Vuilleumier, J. Driver, Modulation of visual processing by attention and emotion:

Windows on causal interactions between human brain regions. *Philos. Trans. R. Soc. B Biol. Sci.* 362, 837–855 (2007).

71. K. McAlonan, J. Cavanaugh, R. H. Wurtz, Guarding the gateway to cortex with attention in visual thalamus. *Nature* 456, 391–394 (2008).

72. D. Sander, D. Grandjean, K. R. Scherer, An Appraisal-Driven Componential Approach to the Emotional Brain. *Emot. Rev.* 10, 219–231 (2018).

73. K. R. Scherer, A. Moors, The Emotion Process: Event Appraisal and Component Differentiation. *Annu. Rev. Psychol.* 70, 719–745 (2019).

74. L. Feldman B., A. B. Satpute, Large-scale brain networks in affective and social neuroscience: Towards an integrative functional architecture of the brain. *Curr. Opin. Neurobiol.* 23, 361–372 (2013).

75. A. Touroutoglou, M. Hollenbeck, B. C. Dickerson, L. Feldman B., Dissociable large-scale networks anchored in the right anterior insula subserve affective experience and attention. *Neuroimage* 60, 1947–1958 (2012).

76. M. Roy, D. Shohamy, T. D. Wager, Ventromedial prefrontal-subcortical systems and the generation of affective meaning. *Trends Cogn. Sci.* 16, 147–156 (2012).

77. E. Meaux, P. Vuilleumier, *Emotion Perception and Elicitation* (Elsevier Inc., 2015).

78. H. Eryilmaz, D. Van De Ville, S. Schwartz, P. Vuilleumier, Lasting Impact of Regret and Gratification on Resting Brain Activity and Its Relation to Depressive Traits. *J Neurosci* 34, 7825–7835 (2014).

79. E. Qiao-Tasserit, *et al.*, Transient emotional events and individual affective traits affect emotion recognition in a perceptual decision-making task. *PLoS One* 12, 1–16 (2017).

80. H. G. Engen, P. Kanske, T. Singer, The neural component-process architecture of endogenously generated emotion. *Soc. Cogn. Affect. Neurosci.* 12, 197–211 (2017).

81. Y. I. Sheline, *et al.*, The default mode network and self-referential processes in depression. *Proc. Natl. Acad. Sci.* 106, 1942–1947 (2009).

82. Z. Song, M. Zhang, P. Huang, Aberrant emotion networks in early major depressive disorder patients: an eigenvector centrality mapping study. *Transl. Psychiatry* 6, e819 (2016).

83. E. J. Liemburg, *et al.*, Altered resting state connectivity of the default mode network in alexithymia. *Soc. Cogn. Affect. Neurosci.* 7, 660–666 (2012).

84. S. Whitfield-gabrieli, J. M. Ford, Default Mode Network Activity and Connectivity in Psychopathology (2012) https:/doi.org/10.1146/annurev-clinpsy-032511-143049.

85. F. Sambataro, N. D. Wolf, M. Pennuto, N. Vasic, R. C. Wolf, Revisiting default mode network function in major depression: Evidence for disrupted subsystem connectivity. *Psychol. Med.* 44, 2041–2051 (2014).

86. J. P. Hamilton, M. Farmer, P. Fogelman, I. H. Gotlib, Depressive Rumination, the Default-Mode Network, and the Dark Matter of Clinical Neuroscience. *Biol. Psychiatry* 78, 224–230 (2015).

87. J.-M. Aubry, *et al.*, Resting-state functional connectivity of emotion regulation networks in euthymic and non-euthymic bipolar disorder patients. *Eur. Psychiatry* 34, 56–63 (2016).

88. J. Joormann, I. H. Gotlib, Emotion regulation in depression: Relation to cognitive inhibition.

Cogn. Emot. 24, 281–298 (2010).

89. B. Abler, *et al.*, Habitual emotion regulation strategies and depressive symptoms in healthy subjects predict fMRI brain activation patterns related to major depression. *Psychiatry Res. - Neuroimaging* (2010) https:/doi.org/10.1016/j.pscychresns.2010.05.010.

90. M. Ertl, M. Hildebrandt, K. Ourina, G. Leicht, C. Mulert, Emotion regulation by cognitive reappraisal - The role of frontal theta oscillations. *Neuroimage* (2013) https:/doi.org/10.1016/j.neuroimage.2013.05.044.

91. M. Uchida, *et al.*, Emotion regulation ability varies in relation to intrinsic functional brain architecture. *Soc. Cogn. Affect. Neurosci.* 10, 1738–1748 (2015).

92. M. W. Cole, *et al.*, Multi-task connectivity reveals flexible hubs for adaptive task control. *Nat. Neurosci.* 16, 1348–1355 (2013).

93. J. R. Andrews-Hanna, J. Smallwood, R. N. Spreng, The default network and self-generated thought: Component processes, dynamic control, and clinical relevance. *Ann. N. Y. Acad. Sci.* 1316, 29–52 (2014).

94. G. B. Chand, J. Wu, I. Hajjar, D. Qiu, Interactions of the Salience Network and Its Subsystems with the Default-Mode and the Central-Executive Networks in Normal Aging and Mild Cognitive Impairment. *Brain Connect.* 7, 401–412 (2017).

95. M. Corbetta, G. L. Shulman, Control of goal-directed and stimulus-driven attention in the brain. *Nat. Rev. Neurosci.* 3, 201–215 (2002).

96. R. N. Spreng, W. D. Stevens, J. D. Viviano, D. L. Schacter, Attenuated anticorrelation between the default and dorsal attention networks with aging: evidence from task and rest. *Neurobiol. Aging* 45, 149–160 (2016).

97. P. Vrtička, G. Bondolfi, D. Sander, P. Vuilleumier, The neural substrates of social emotion perception and regulation are modulated by adult attachment style. *Soc. Neurosci.* 7, 473–493 (2012).

98. M. L. Dixon, *et al.*, Heterogeneity within the frontoparietal control network and its relationship to the default and dorsal attention networks. SI. *Proc. Natl. Acad. Sci.* 115, E1598–E1607 (2018).

99. J. Pan, *et al.*, Emotion Regulation and Complex Brain Networks: Association Between Expressive Suppression and Efficiency in the Fronto-Parietal Network and Default-Mode Network. *Front. Hum. Neurosci.* 12, 1–12 (2018).

100. C. B. Young, *et al.*, Dynamic Shifts in Large-Scale Brain Network Balance As a Function of Arousal. *J. Neurosci.* 37, 281–290 (2017).

101. S. N. Garfinkel, H. D. Critchley, O. Pollatos, The interoceptive system: Implications for cognition, emotion, and health. *Handb. Psychophysiology, Fourth Ed.*, 427–443 (2016).

Supplementary Information for

Functional dynamics of brain networks associated with carry-over effects of negative events on subsequent resting state.

Julian Gaviria *[a,b,c, 1]. ORCID ID: 0000-0002-4266-1371

Gwladys Rey [c]. ORCID ID: 0000-0001-7192-1577

Thomas Bolton [d,e]. ORCID ID: 0000-0002-2081-4031

Dimitri Van De Ville [d,e]. ORCID ID: 0000-0002-2879-3861

Patrik Vuilleumier [a,b,c]. ORCID ID: 0000-0002-8198-9214

[a]Laboratory for Behavioral Neurology and Imaging of Cognition; [b]Department of Fundamental Neurosciences, University of Geneva, Geneva, Switzerland; [c] Swiss center for Affective Sciences, University of Geneva; [d]Medical Image Processing Lab, Institute of Bioengineering/Center for Neuroprosthetics, École Polytechnique Fédérale de Lausanne (EPFL), Geneva, Switzerland; [e]Department of Radiology and Medical Informatics, University of Geneva, Geneva, Switzerland

* Correspondence mail: jualgalo@gmail.com

Experimental data

A subset of data concerning the fMRI recording of resting periods was previously reported in (1), where our analysis was exclusively focused on dFC patterns in resting periods following both affective and cognitive stimulation conditions. The present work includes both fMRI and behavioral data from the audiovisual affective induction, not considered in the previous study, and conversely does not include rest periods following cognitive task performance. Both data subsets were collected in the same fMRI session.

Affective stimuli

A well validated videoclip with strong emotional content was used to modulate affective state. This clip was edited from the film "*21 Grams*" (2), used in previous mood induction studies (3, 4) and more recently in (5). The excerpt included a young mother as main character, experiencing the loss of her underage children. We reinforced a first-person perspective by recruiting only female participants, and instructed them to feel involved while watching the movie clip. In addition, a neutral clip of 5-minutes was taken from a TV documentary freely available in the internet, with verbally interacting people generally similar to the sad movie but without any strong emotional aspect. The free software iMovie (https://www.apple.com/lae/imovie/) was used for editing the movies. This resulted in a set of 2 clips of 5 min each that were validated in a preliminary pilot study, where a different group of healthy volunteers (n=28) rated the pleasantness, intensity, and type of emotions elicited by each movie. The final clips were compared in terms of low-level features (sound level, luminance, spatial frequency and motion), and no significant differences between both conditions were found.

Subjective emotional measurements

Mood questionnaires assessing the participant's affective state were given before and after each experimental context, including the Positive and Negative Affect Scales, PANAS (Watson et al., 1988). Additionally, participants rated their affective response to each movie with a 9-point Likert scale combined with the self-assessment Manikin, SAM (7), as used in previous work (Borchardt et al., 2017; Hanich et al., 2014). These ratings included valence ("How happy/pleased or unhappy/dissatisfied are you?", 1 = very unhappy, 9 = very happy), arousal ("How awake/aroused or calm/drowsy do you feel?" ,1 = very calm, 9 = very aroused), and subjective hedonic experience ("How pleasant or unpleasant was your own experience of the scene?",1 = very unpleasant, 9 = very pleasant). Full results are described in Figure 1B.

FMRI data acquisition

Neuroimaging data were collected using a 3T Magnetom TIM Trio scanner (Siemens, Germany) and a 32 channels head-coil. The Blood Oxygenation Level Dependent (BOLD) contrast was measured using a T2*-weighted echo-planar sequence (EPI). 928 functional volumes of 36 axial slices each (TR/TE/flip angle = 1300ms/30ms/80°, FOV=192 mm, resolution=64×64, isotropic voxels of 3.2 mm^3, distance factor 20%) were acquired in one single continuous scanning run for each scanning session. We collected a high-resolution T1-weighted anatomical image (TR/TI/TE/flip angle=1900ms/900ms/2.27ms/9°, FOV=230mm, resolution=256×256, slice thickness=0.9mm, 192 sagittal slices) at the end of the first session.

Preprocessing for GLM-based fMRI analysis

Standard image preprocessing procedures were applied using SPM12 (www.fil.ion.ucl.ac.uk/spm/). Functional images were realigned, slice-time corrected, normalized, and co-registered to individual skull stripped anatomical images comprising probabilistic maps of CSF (cerebrospinal fluid), gray, and white matter extracted by the DARTEL Algorithm (8). Data was spatially smoothed with an 8 mm Gaussian kernel for GLM analysis and 5 mm for CAP analysis.

GLM-based fMRI analysis

Data from the movie and resting blocks were analyzed using the General Linear Model as implemented in SPM12. Four GLM boxcar regressors represented each experimental condition (i.e., neutral movie, neutral rest, negative movie, and negative rest respectively). These regressors were convolved with a standard hemodynamic response function (HRF) according to a blocked design, which was then submitted to a univariate regression analysis. Realignment parameters were added to the design matrices of both models, to account for any residual movement confounds. In all cases, the design matrix included low-frequency drifts (cutoff frequency at 1/128 Hz). Flexible factorial analyses of variance (ANOVAs) were then performed on the main contrasts of interest. All statistical analyses were carried out at the whole-brain level, with a threshold at $P < 0.05$, FWE corrected at whole brain level (unless specified otherwise). A first contrast inspected the BOLD response between the movies (negative movie > neutral movie) and another compared the resting periods (negative rest > neutral rest). This GLM analysis was used to define ROIs as seeds for the main CAP analysis.

Preprocessing for co-activation pattern (CAP) analysis

Following Bolton et al., (9) standard image preprocessing procedures were applied using the DPABI toolbox (10). Time-series from each seed ROI in the white matter and cerebrospinal fluid, plus the six affine motion parameters from realignment (including their respective first-order derivatives), were used as nuisance variables to be regressed out from the data. No global signal regression was carried out given the absence of agreement in the field, particularly on this regard (11). Furthermore, the data were band-pass filtered between 0.01 and 0.10 Hz. All image volumes with frame-wise displacement above 0.5 mm were discarded, as well as subjects with more than 50% of scrubbed frames (12). Less than 5% of the total time frames were scrubbed and estimated with cubic spline interpolation, in order to avoid alterations in the signal's temporal continuity or producing additional artifacts (13, 14). However, removing corrupted frames before further analyses has less impact in the CAPs methodology compared to other dFC methods, due to the CAPs' single-volume temporal resolution and minimal set of assumptions (15).

Tests for comparing CAPs correlations.

Occurrences of relevant CAPs were compared by correlations performed on the same CAP (within-CAP analysis) and across different CAPs (between-CAPs analysis) with the R-based cocor package [version 1.1-0 (16)] with the formula described below.

Within-CAPs analyses involved the comparison of two overlapping correlations [e.g., $DMN_{neutral\ movie}$ - $DMN_{neutral\ rest}$; vs. $DMN_{neural\ movie}$ - $DMN_{negative\ rest}$) based on dependent groups (e.g., these correlations include only data from the DMN-CAP). As a consequence, we applied the function "cocor.dep.groups.overlap()" of the cocor package to compute correlation values (e.g., $DMN_{neutral\ movie}$ - $DMN_{neutral\ rest}$= *rjk*) and ($DMN_{neutral\ movie}$ - $DMN_{negative\ rest}$= *rjh*) that were then compared by the Zou's confidence interval test (17). If the confidence interval includes zero, the null hypothesis that the two correlations are equal must be retained. If zero is outside the confidence interval, the null hypothesis has to be rejected. A lower and upper bound for the interval (L and U, respectively) is given by

$$L = r_{jk} - r_{jh} - \sqrt{(r_{jk} - l_1)^2 + (u_2 - r_{jh})^2 - 2c(r_{jk} - l_1)(u_2 - r_{jh})} \quad [1]$$

and

$$U = r_{jk} - r_{jh} - \sqrt{(u_1 - r_{jk})^2 + (r_{jh} - l_2)^2 - 2c(u_1 - r_{jk})(r_{jh} - l_2)} \quad [2]$$

(17) where

$$l = \frac{exp(2l') - 1}{exp(2l') + 1`} \quad [3]$$

$$u = \frac{exp(2u') - 1}{exp(2u') + 1}$$

(17)

$$c = \frac{\left(r_{kh} - \frac{1}{2} r_{jk} r_{jh}\right)\left(1 - r_{jk}^2 - r_{jh}^2 - r_{jk}^2\right) + r_{kh}^2}{(1 - r_{jk}^2)(1 - r_{jh}^2)} \quad [4]$$

(17) and

$$l', u' = Z \pm z \frac{\alpha}{2} \sqrt{\frac{1}{n-3}} \quad [5]$$

(17) α denotes the desired alpha level of the confidence interval, whereas n specifies the size of the group the correlation is based on.

Between-CAPs analyses involved comparisons of correlations [e.g., $DMN_{neutral\ movie}$ - $FPCN_{neutral\ rest}$; vs. $DMN_{negative\ movie}$ - $FPCN_{negative\ rest}$) based on dependent groups (e.g., occurrences from DMN-CAPs and FPCN-CAPs respectively). We therefore used the function "cocor.dep.groups.nonoverlap.()" to compute these correlations (e.g., $DMN_{neutral\ movie}$ - $FPCN_{neutral\ rest}$= r_1) and ($DMN_{negative\ movie}$ - $FPCN_{negative\ rest}$= r_2) and then compared them by the Zou's confidence interval test (17). If the confidence interval includes zero, the null hypothesis that the two correlations are equal must be retained. If zero is outside the confidence interval, the null hypothesis has to be rejected. A lower and upper bound for the interval (L and U, respectively) is given by

$$L = r_1 - r_2 - \sqrt{(r_1 - l_1)^2 + (u_2 - r_2)^2} \quad [6]$$

and

$$U = r_1 - r_2 - \sqrt{(u_1 - r_1)^2 + (r_2 - l_2)^2} \quad [7]$$

(17) A lower and upper bound for the confidence interval of r1 (l1 and u1) and r2 (l2 and u2) are calculated as

$$l = \frac{exp(2l') - 1}{exp(2l') + 1`} \quad [8]$$

$$u = \frac{exp(2u') - 1}{exp(2u') + 1}$$

(17) where

$$l', u' = Z \pm z\frac{\alpha}{2}\sqrt{\frac{1}{n-3}} \quad [9]$$

(17) α denotes the desired alpha level of the confidence interval, whereas n specifies the size of the group the correlation is based on.

Supplementary Results

Psychological indices of emotion elicitation

As expected, subjective affective ratings following the negative and neutral movies yielded significant differences. Valence was more negative for the sad than neutral clip [F (1, 72) = 3.97, p < .01] (Fig. 1), and arousal was higher [F (1, 72) = 3.96, p < .01]. Subjective emotional experience (Likert scale from 1 to 9) was also rated as more negative after watching the sad than the neutral movie [F (1, 72) = 3.97, p < .01] (see Fig. 1B). Likewise, the PANAS questionnaire indicated a significant difference in subjective affect before and after exposure to movies in the "negative" context, with higher negative affect (NA) scores [**t (**18**) =** 1.7**, p <** 0.01] and, lower positive affect (PA) scores [**t (**18**) >** 1.7**, p <** 0.05] in the post scan ratings (see Fig. 3B). Such differences between pre and post scanning were not observed for the "neutral" context [**t (**18**) >** 1.7**, p >** 0.1] (Fig. 3A).

Results of CAP analysis with insula-based and precuneus based seeds

Based on the data-driven consensus procedure used for our CAP analysis, we found a set of 7 distinct networks co-activating with the insula during movie periods and another set of 7 networks co-activating with the precuneus during rest periods. These networks overlap with IFNS commonly reported in the literature (54–56) are shown in Fig. S2.2.

Among CAPs connecting with the precuneus, CAP1 overlapped with a typical visual network (20), while CAP2, CAP4, and CAP5 included fronto-parietal areas commonly associated with the dorsal attention network (DAN) and the central executive control network (CEN) (21, 22). CAP3 showed a high similarity to DMN (19), encompassing medial prefrontal, posterior cingulate, and inferior parietal cortices. CAP6 involved several brain regions implicated in social cognition such as STS and TPJ, and CAP7 was centered on primary sensorimotor areas.

CAPs connecting with the insula comprised networks associated with visuo-spatial attention processes (CAP1), somatosensory and motor functions (CAP2, CAP3, CAP6), anterior dorsomedial prefrontal areas (CAP4) and posterior occipito-cingulate areas (CAP7), as well as fronto-parieto-cingulate areas (CAP5) that resembled the frontoparietal control network (18).

Results from statistical analysis comparing the occurrence rate of all CAPs across experimental conditions are shown in Fig S2.2. Only four CAPS showed a significant modulation by condition type, and these were therefore considered for our main analysis (see main text and Fig. 2).

Supplementary figures

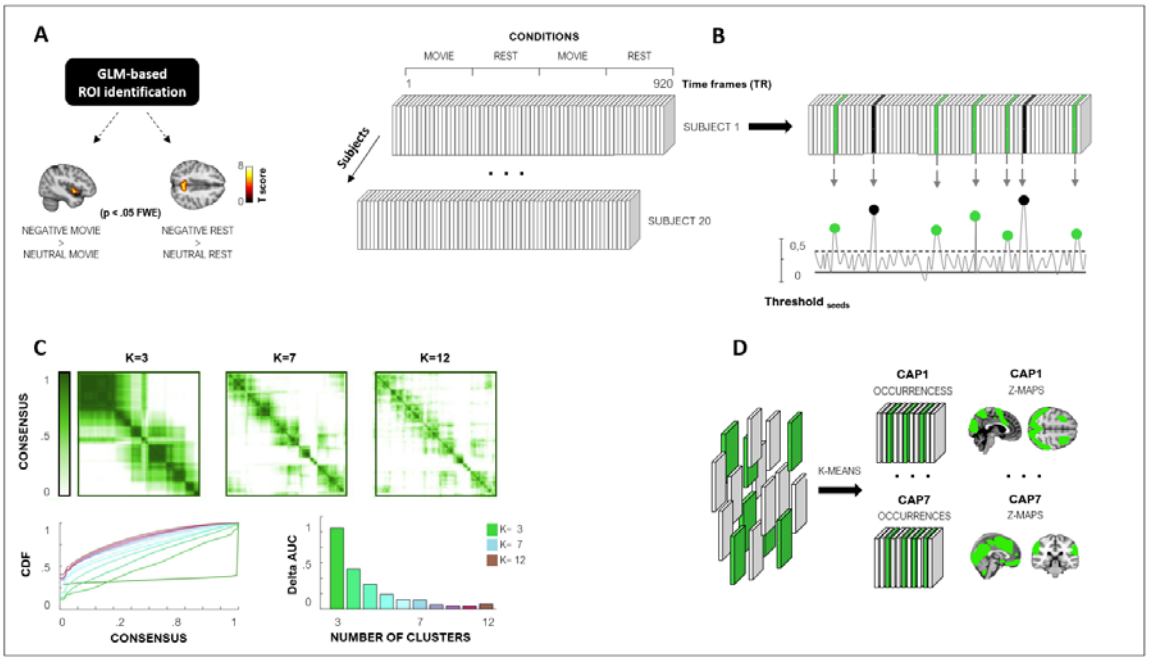

Figure S1. Co-activation patterns (CAPs) analyses pipeline. **A)** Regions of interest (ROIs) in insula (movie-related) and precuneus (rest-related) were used for two different CAP analyses and identified by a preliminary GLM analysis. The left insula was defined by the contrast "negative movies" > "neutral movies", while the precuneus was defined by the contrast "negative rest > "neutral rest" ($p<.05$ FWE). **B)** The activity time-course from each seed was computed separately for each subject across all experimental blocks, and the frames for which it exceeded a positive threshold $T_{seed} = 0.5$ (green) were tagged. Frames corrupted by framewise displacement (0.5 mm) were also tagged (black) and removed from analysis. **C)** A consensus resampling-based clustering algorithm was implemented to obtain the number and membership (consensus) of reliable CAPs within our dataset. Parameters used to calculate the ''consensus rate'' between all pairs of samples included 80% of item resampling, a maximum k of 12, and 50 resamplings, with Euclidean distance indices as the distance measurement. Up: Heatmaps of consensus matrices for k=3, k=7, k=12, where values range from 0 (samples are never clustered together across consensus folds) to 1 (always clustered together), marked by white to dark red colors. Bottom left: Consensus Cumulative Distribution Function (CDF) of the consensus matrices from k = 2 to k = 12 (k=3, k=7, and k=12; indicated by green, clear blue, and brown, respectively), describing how consensus entries distribute for each case. Bottom right: Delta area under the curve plot, indicating the relative change in area under the CDF curve (a larger area change implies a larger increase in the quality of clustering at the assessed k). These results provide qualitative (top matrices) and quantitative (bottom plots) information suggesting that k = 7 is the optimal number of clusters for classifying our fMRI rest dataset. **D)** K-means clustering. Retained frames across subjects (depicted by different shades of green) undergo k-means clustering to be separated into K different co-activation patterns (CAPs), each defined as the arithmetic mean between the subset of frames denoting one particular network of regions (voxelwise), with which the seed was strongly co-active. A detailed review on the CAP methodology is found in (15); and further description of the tbCAPs toolbox is provided in (9)

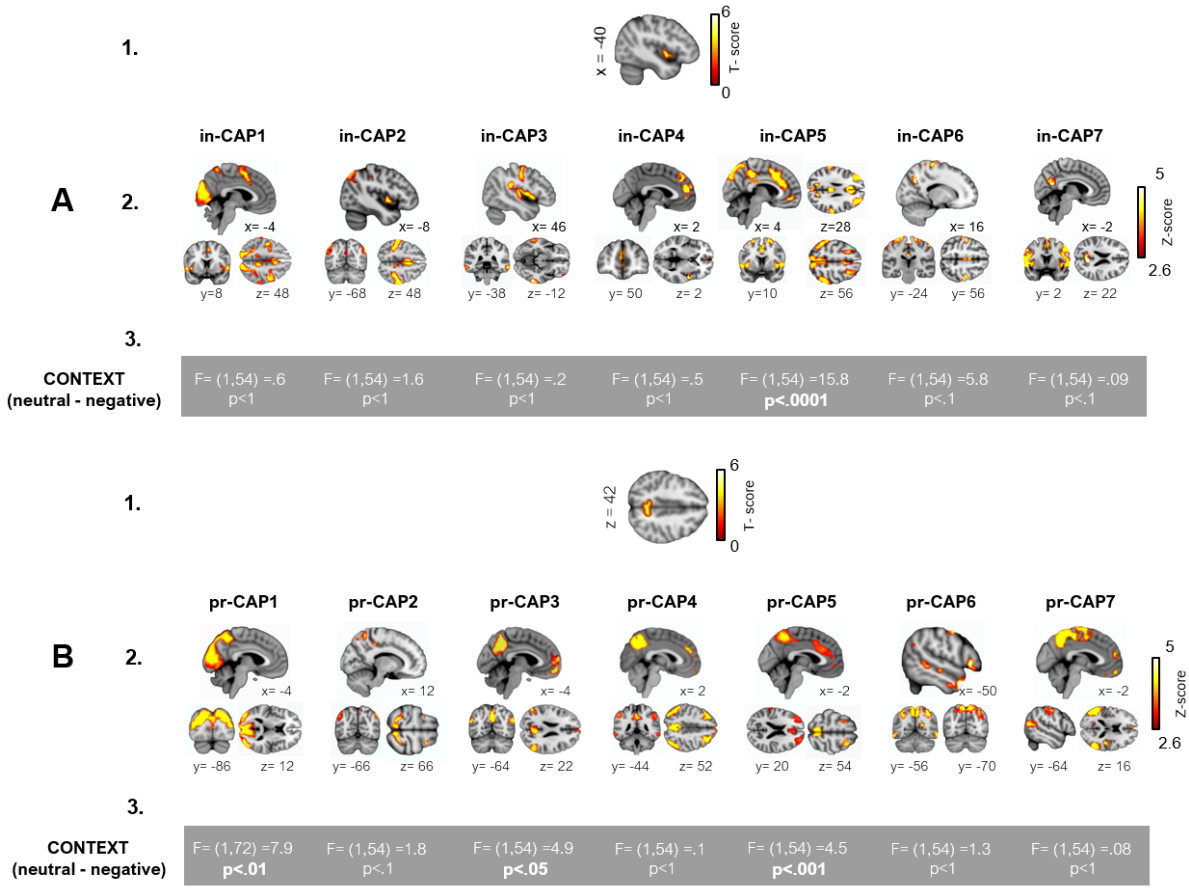

Figure S2. Results of the co-activation pattern analyses. A. Brain networks functionally connected to insula. **A1.** Insula seed determined by preliminary GLM contrasting fMRI data recorded during movies (i.e., "negative movie" > "neutral movie"). **A2.** Illustration of the 7 CAPs found to be most reliably co-active with the left insula ("in"-CAPs) across all experimental conditions. **A3.** Results of the gLMM-factorial analyses showing a main effect of affective "contexts" (i.e., neutral vs negative) for the same networks. **B.** Similar analysis for networks connected with precuneus. **B1.** Seed in precuneus determined by preliminary GLM contrasting fMRI data during resting periods ("negative rest" > "neutral rest"; see "Methods" section). **B2.** Illustration of the 7 CAPs found to be most reliably co-active with precuneus ("pr"-CAPs) across all experimental conditions. **B3.** Results of gLMMs on the occurrences for each of these (pr)CAP across conditions. Statistical analyses highlighted significant main effects of "affective context" in occurrences for pr-CAP1, pr-CAP3, pr-CAP5, and in-CAP5 in the 2x2 factorial analysis. Anatomical information on these four affectively relevant CAPs is provided in Table S1. Full statistical results are reported in Table S2.

REGION (MNI)	X	Y	Z	K>	Z MAX.
VIS-CAP					
Precuneus	-2	-54	54	347	4.2
Cuneus	4	-84	24	28	3.3
Middle occipital gyrus (L)	-22	-88	24	946	4.1
Middle occipital gyrus (R)	24	-88	26	782	4.3
Lingual gyrus (R)	20	-68	-4	255	3.8
Lingual gyrus (L)	-18	-70	-4	48	3.1
DMN-CAP					
Precuneus	4	-62	38	503	4.8
Middle temporal gyrus (L)	-52	-70	30	163	3.4
Superior temporal gyrus. (R)	54	-58	22	251	3.7
Medial frontal gyrus (B)	4	58	-8	205	3.6
CEN-CAP					
Middle frontal gyrus (L)	-28	36	34	210	3.5
Middle frontal gyrus (R)	30	40	36	253	3.7
Middle cingulate gyrus (B)	2	20	34	309	3.1
Precuneus (B)	-2	-52	52	613	5.0
FPCN-CAP					
Precuneus (L)	-10	-70	32	644	3.2
Middle cingulate gyrus (B)	4	-34	46	321	3.1
Anterior cingulate gyrus (B)	-2	22	24	712	3.6
Orbital medial frontal gyrus (R)	2	46	-6	43	2.3
Inferior parietal lobule (L)	-42	-48	48	1139	2.8
Insula (R)	42	14	-4	831	3.2
Insula (L)	-42	8	-4	813	3.6
Inferior parietal lobule (R)	56	-40	48	1186	3.6

Table S1. Spatial maps of the affectively relevant CAPs. Activity peaks obtained for the precuneus-based CAP analysis (VIS-CAP1, DMN-CAP3, CEN-CAP5) and the insula-based CAP analysis (FPCN-CAP5). Brain regions consistently co-activating with these seeds are reported after thresholding at $z > 2.58$ (equivalent to $p<.01$).

	GLMMs FACTORIAL ANOVA			LS MEANS	
CAP	**CONTEXT** NEU. – NEG.	**PERIOD** MOVIE – REST	**INTERACTION** EVENT X CONTEXT	**CONTRASTS**	P_{FDR}
in-FPCN	F= (1,54) = 15.8 P_{FDR}<.001	F= (1,54) = 46.6 P_{FDR}<.0001	F= (1,54) = 4.5 P_{FDR} <.05	NEG. MOVIE > NEU. MOVIE	<.001
				NEG. MOVIE > NEU. REST	<.001
				NEG. MOVIE > NEG. REST	<.0001
pr-VIS	F= (1,54) = 7.9 P_{FDR}<.01	F= (1,54) = 4.4 P_{FDR}<.05	F= (1,54) = 2.1 P_{FDR}<.1	NEG. MOVIE > NEU. MOVIE	<.01
				NEG. MOVIE > NEU. REST	<.01
				NEG. MOVIE > NEG. REST	<.001
pr-DMN	F= (1,54) = 4.9 P_{FDR}<.05	F= (1,54) = 2.2 P_{FDR}<.1	F= (1,54) = 0.1 P_{FDR}<1	NEG. REST > NEU. MOVIE	<.001
				NEG. REST > NEU. REST	<.05
				NEG. REST > NEG. MOVIE	<.01
pr-CEN	F= (1,54) = 4.5 P_{FDR}<.001	F= (1,54) = 7.0 P_{FDR}<.0001	F= (1,54) = 10.2 P_{FDR}<.001	NEU. MOVIE > NEU. REST	<.0001
				NEU. MOVIE > NEG. MOVIE	<.001
				NEU. MOVIE > NEG. REST	<.001

Table S2. Results of GLMMs analyses on temporal occurrences of relevant / emotion-sensitive CAPs. Statistical results of a 2x2 factorial assessment of the "context" (neutral vs. negative), and "period" (movies vs. rest) effects on CAPs occurrences. Significant post hoc pairwise contrasts driving main effects and interactions are listed in the right-hand columns., this factorial analysis revealed that 4 out of the 14 brain networks identified in our CAP analysis (see full description in Fig. S2) exhibited a distinctive activity profile according to our experimental conditions. These four relevant CAPs were therefore selected for all main analyses in our study. Multiple testing was corrected for multiple comparisons by applying the FDR (false discovery rate) method under dependency (see methods).

INTRA-CAPS COMPARISONS

CONTRASTS (r)	CAP	Z-SCORE	P-VALUE	CI	
NEU. MOVIE – NEU. REST	VIS	0,35	0,73	-0,44	0,61
VS.	DMN	1,09	0,28	-0,24	0,75
NEG. MOVIE – NEG. REST	CEN	-0,07	0,95	-0,57	0,55
	FPCN	-0,02	0,99	-0,56	0,56
NEU. MOVIE – NEU. REST	VIS	-0,57	0,58	-0,84	0,51
VS.	DMN	-0,71	0,48	-0,85	0,45
NEU. MOVIE – NEG. REST	CEN	0,72	0,48	-0,47	0,9
	FPCN	0,77	0,44	-0,49	0,97
NEU. MOVIE – NEU. REST	VIS	-0,89	0,39	-0,93	0,39
VS.	DMN	-1,12	0,26	-0,92	0,32
NEG. MOVIE – NEU. REST	CEN	0,17	0,87	-0,66	-0,28
	FPCN	0,77	0,45	-0,45	0,89
NEG. MOVIE – NEG. REST	VIS	-1,21	0,23	-1,01	0,32
VS.	**DMN**	-2.35	**0,02**	-1,16	-0,03
NEG. MOVIE – NEU. REST	CEN	-0,22	0,83	-0,78	0,65
	FPCN	0,7	0,49	-0,52	0,95
NEG. MOVIE – NEG. REST	VIS	-0,88	0,38	-0,89	0,39
VS.	**DMN**	-2,05	**0,04**	-1,14	0,04
NEU. MOVIE – NEG. REST	CEN	0,77	0,44	-0,46	0,91
	FPCN	-0,84	0,4	-0,91	0,43

Table S3. Intra-CAPs comparisons. Comparison of intra-CAP functional relationships (correlation of occurrences during movie with occurrences during rest) between the two emotional conditions, for each CAP of interest. Intra-CAPs correlations between DMN_{movie} and DMN_{rest} were significantly different only in the negative affect context. See graphical illustration of DMN (r) comparisons in Fig. 4. Multiple testing and dependency of the correlations was considered and corrected when their comparisons included overlapping variables (e.g., intra-CAP contrast: $DMN_{neutral\ movie}$ - $DMN_{neutral\ rest}$ vs. $DMN_{neutral\ movie}$ - $DMN_{negative\ rest}$).

Supplementary References

1. J. Gaviria, *et al.*, Brain functional connectivity dynamics at rest in the aftermath of affective and cognitive challenges. *Hum. Brain Mapp.*, hbm.25277 (2020).

2. A. González Iñárritu, 21 Grams (Universal pictures, 2003).

3. J. Hanich, V. Wagner, M. Shah, T. Jacobsen, W. Menninghaus, Why we like to watch sad films. The pleasure of being moved in aesthetic experiences. *Psychol. Aesthetics, Creat. Arts* 8, 130–143 (2014).

4. M. N. Shiota, R. W. Levenson, Effects of aging on experimentally instructed detached reappraisal, positive reappraisal, and emotional behavior suppression. *Psychol. Aging* 24, 890–900 (2009).

5. V. Borchardt, *et al.*, Echoes of Affective Stimulation in Brain connectivity Networks. *Cereb. Cortex* 28, 4365–4378 (2018).

6. D. Watson, L. A. Clark, A. Tellegen, Development and Validation of Brief Measures of Positive and Negative Affect: The PANAS Scales. *J. Pers. Soc. Psychol.* 54, 1063–1070 (1988).

7. M. Bradley, P. J. Lang, Measuring Emotion: The Self-Assessment Semantic Differential Manikin and the. *J. Behav. Ther. Exp. Psychiatry* 25, 49–59 (1994).

8. J. Ashburner, A fast diffeomorphic image registration algorithm. *Neuroimage* 38, 95–113 (2007).

9. T. A. W. Bolton, *et al.*, TbCAPs: A toolbox for co-activation pattern analysis. *Neuroimage* 211, 116621 (2020).

10. C. G. Yan, X. Di Wang, X. N. Zuo, Y. F. Zang, DPABI: Data Processing & Analysis for (Resting-State) Brain Imaging. *Neuroinformatics* (2016) https:/doi.org/10.1007/s12021-016-9299-4.

11. K. Murphy, M. D. Fox, Towards a consensus regarding global signal regression for resting state functional connectivity MRI. *Neuroimage* 154, 169–173 (2017).

12. J. D. Power, *et al.*, Methods to detect, characterize, and remove motion artifact in resting state fMRI. *Neuroimage* 84, 320–341 (2014).

13. H. Chen, J. S. Nomi, L. Q. Uddin, X. Duan, H. Chen, Intrinsic functional connectivity variance and state-specific under-connectivity in autism. *Hum. Brain Mapp.* (2017) https:/doi.org/10.1002/hbm.23764.

14. R. M. Hutchison, *et al.*, Dynamic functional connectivity: Promise, issues, and interpretations. *Neuroimage* 80, 360–378 (2013).

15. X. Liu, N. Zhang, C. Chang, J. H. Duyn, Co-activation patterns in resting-state fMRI signals. *Neuroimage*, 1–10 (2018).

16. B. Diedenhofen, J. Musch, Cocor: A comprehensive solution for the statistical comparison of correlations. *PLoS One* 10, 1–12 (2015).

17. G. Y. Zou, Toward using confidence intervals to compare correlations. *Psychol. Methods* 12, 399–

413 (2007).

18. M. W. Cole, G. Repovš, A. Anticevic, The frontoparietal control system: A central role in mental health. *Neuroscientist* 20, 652–664 (2014).

19. J. R. Andrews-Hanna, J. S. Reidler, J. Sepulcre, R. Poulin, R. L. Buckner, Functional-Anatomic Fractionation of the Brain's Default Network. *Neuron* 65, 550–562 (2010).

20. P. A. Kragel, M. C. Reddan, K. S. LaBar, T. D. Wager, Emotion schemas are embedded in the human visual system. *Sci. Adv.* 5 (2019).

21. P. S. GOLDMAN-RAKIC, Architecture of the Prefrontal Cortex and the Central Executive. *Ann. N. Y. Acad. Sci.* 769, 71–84 (1995).

22. V. Menon, L. Q. Uddin, Saliency, switching, attention and control: a network model of insula function. *Brain Struct. Funct.* 214, 655–667 (2010).